Integrity of Glass-reinforced Plastic (GRP) Vessels under Ice Loading

by

© Md Samsur Rahman

A thesis submitted to the School of Graduate Studies

in partial fulfillment of the requirements for the degree of

Master of Engineering

Faculty of Engineering and Applied Science

Memorial University of Newfoundland

May 2015

St. John's   Newfoundland   Canada

ABSTRACT

Small glass-reinforced plastic (GRP) vessels, such as lifeboats and fishing vessels are occasionally used in sea ice conditions, despite the lack of structural design standards and operating standards for such conditions. In addition, there is limited knowledge relating to the magnitude of local ice loads on these vessels or the structural integrity of these craft under ice loading. To address these gaps, full-scale measurements relating to lifeboat-ice interactions were collected during a field campaign carried out in 2013 and 2014. During these trials, the local ice loads on the hull of a Totally Enclosed Motor Propelled Survival Craft (TEMPSC) operating in pack ice conditions were measured using instrumented load panels. This full-scale field data provides the foundation for risk-based design load estimation and has been analyzed using the event-maximum method of local ice pressure analysis. This approach is based on probabilistic methods developed for the analysis of ice loads measured on icebreakers, which have been adapted for ice interaction scenarios involving small vessels. Results from this work provide improved understanding into the nature of loads on small GRP vessels operating in ice-covered waters and help to inform design methodology for these vessels. To compliment these results, the field trials were also assessed in terms of the operational methods used by different coxswains when maneuvering through an ice field. Insights from this analysis provide operational guidance towards methods that can mitigate peak impacts and improve the maneuverability of these vessels in ice.

To

my parents

&

my sister, Nazmun

ACKNOWLEDGEMENTS

Table of Contents

List of Tables

List of Figures

List of Symbols and Abbreviations

Symbols

a Panel area

α Parameter that defines the dependence of pressure on contact area

η Weibull scale parameter

β Weibull shape parameter

r Expected proportion of impacts on a given region

v Expected number of events

x Random quantity denoting pressure

x_0 Parameter of a pressure curve that represents exposure

z_e Extreme pressure

C_H High ice concentration

C_L Low ice concentration

C_M Medium ice concentration

C, D Empirical constants that relate the ice pressure to the nominal contact area

EL   Lifeboat operators with experience in ice

$F_Z(z_e)$ Exceedance probability

LV   Large vessel operators

P_e Plotting position

PL   Path length

SA   Sail-away distance

SC   Small craft operators

Abbreviations

COG   Course Over Ground

DAS   Data Acquisition System

DGPS   Differential Global Positioning System

EER   Escape, Evacuation and Rescue

FRC   Fast Response Craft

GRP   Glass-reinforced Plastics

ISO   International Standards Organization

LSA   Life-Saving Appliances

LVDT   Linear Variable Differential Transformer

NRC   National Research Council

PIC   Programmable Interface Controllers

SOLAS   Safety of Life at Sea

TEMPSC   Totally Enclosed Motor Propelled Survival Craft

1 Introduction

1.1 Background

Small vessels made from composite materials (glass-reinforced plastics), such as lifeboats and fishing vessels, are used on occasion in sea ice conditions. These small craft are designed for temperate regions that do not contain ice. Their fiberglass hulls are adequate in open water conditions, but there is a lack of design and operating standards that consider ice conditions. In addition, there is a lack of information relating to the durability of marine composite hulls subject to various ice loads while transiting through prevailing ice conditions under power. Compared to the high strength steel typically used in larger ice-going vessels, the composite materials used in lifeboats and similar small vessels are very flexible, which means that the ice-structure interaction between the composite structure and ice is markedly different than what occurs with stiff steel structures.

The use of small composite vessels in more severe ice conditions is anticipated to increase in the coming years, as the offshore petroleum and minerals industries explore for and develop resources in northern frontiers. Existing types of marine evacuation systems, which are mandatory on vessels and offshore petroleum installations, may not have the required capabilities to operate in some ice conditions because of their low hull strength and limited icebreaking capability. Regulations and standards (e.g. ISO, 2011) define the broad performance goals of escape, evacuation and rescue systems, but do not offer any detailed design guidance related to the structural strength of lifeboat hulls during ice loading.

1.2   Aim and Scope of Work

The aim of this thesis work is to provide technical guidance relevant to the design of composite structures for small vessels that operate in pack ice conditions, as well as guidance on operating procedures for composite vessels that operate in ice. The key goals of this work are:

1. Develop a methodology to improve the level of understanding relating to ice loading on small composite vessels and provide design guidance for these vessels in ice conditions

2. Provide insights to improve the operational performance of small composite vessels operating in ice

An important starting point for this work is a full-scale data set acquired during field trials campaigns carried out in 2013 and 2014. During these trials, the local ice loads on the hull of a TEMPSC operating in pack ice conditions were measured using instrumented load panels (Kennedy et al., 2014; Rahman et al., 2014). This full-scale field data provides the foundation for risk-based design load estimation and has been analyzed using the event-maximum method of local ice pressure analysis (Jordaan et al., 1993; Taylor et al., 2010). This probabilistic approach formed the basis for establishing risk-based design criteria, relevant to lifeboats and other small GRP vessels, which adequately represents the ice conditions encountered during the entire design life of the vessel. Further, an investigation of the effect of operational factors, such as different operating

styles and coxswain experience, on the performance of lifeboats in terms of the magnitude of ice loads, the vessel's motions, and the transit distance was performed. This investigation was conducted in an attempt to identify any operational means to improve the performance of these types of vessels in ice environments.

1.3 Organization of the Thesis

This thesis is composed of six chapters. The first chapter addresses the general background, aim, and the scope of the proposed research work. Chapter 2 covers a literature review relevant to Arctic escape, evacuation and rescue (EER) and existing ice load modeling methods. Chapter 3 describes the details of the full scale field experiments that were conducted with the lifeboat in pack ice conditions. This chapter also provides a description of the data collected during these field tests, which was analyzed and described further in subsequent chapters. Chapter 4 provides a description of the analysis of ice loads using the event-maximum method and how this tool can be used to provide guidance towards design load estimation. This chapter also presents the operational ice load models for various ice conditions, based on the presented analysis methodology. Chapter 5 describes the effects of selected operational parameters on the performance of a lifeboat in ice conditions. Finally, Chapter 6 summarizes the original contributions of this thesis along with some guidelines for future work.

2 Literature Review

Research has been performed to inform the structural and operational guidelines for icebreaking ships operating in ice-covered regions. Some of this work might be relevant to the phenomena involved in lifeboats and other small GRP vessels operating in ice. Ice-structure interaction is significantly different between icebreaking ships and lifeboats due to variations in total kinetic energy, hull-material type, and bow configuration. In addition, the purpose of using icebreakers and lifeboats is not the same as lifeboats are not meant for breaking or clearing the ice. Therefore, emphasis is placed on the study of lifeboat-ice interaction to gain better understanding on design and operational performance of these small boats in ice.

Simões Ré and Veitch (2008) described the goals and expectations of EER on offshore petroleum installations and ships in cold regions. Credible hazards, the physical environment, people, and installation design and equipment were identified as the key factors of emergency EER response and the interaction of these factors were presented. There is no unique solution for evacuation and rescue; rather it was suggested to design evacuation and rescue assets by considering the characteristics of different sites. Wright et al. (2002, 2003) presented an overview of the issues related to the safe evacuation of personnel from offshore structures in ice. This report identified the challenges regarding the launching and operation of conventional lifeboats in ice-covered water. Loads are a very strong function of the impact velocity and the shape of the bottom of the lifeboat during the deployment of the lifeboat in ice-covered water. Alternative modes of

evacuation in ice have been proposed by Seligman et al. (2008), Johansson (2006), Browne et al., (2008). Seligman et al. (2008) presented the reliability of the ARKTOS, an amphibious evacuation craft that was designed for operation in a wide range of Arctic ice conditions and sea-states. Johansson (2006) and Browne et al. (2008) proposed design ideas for ice strengthened lifeboats.

Several lifeboat model test campaigns were performed by Simões Ré and Veitch (2003), Simões Ré and Veitch (2007), Barker et al. (2004), Lau and Simões Ré (2006). Simões Ré and Veitch (2003) investigated the performance capabilities of a conventional lifeboat at model scale in a range of ice concentrations, piece sizes, and thicknesses. The lifeboat was able to progress through ice concentrations of up to 7/10ths coverage in the thinner ice and smaller floes. In the thicker ice and larger floes, ice concentrations of only 5/10ths were passable by the lifeboat. Simões Ré and Veitch (2007), and Simões Ré et al. (2006) described a series of model scale experiments to examine effects of three different hull forms and propulsive power. In terms of ice conditions, concentrations of 6/10ths to 8/10ths were found to be impassable and the limit was reached at lower ice concentrations for thicker and larger ice pieces. Significant increases in powering slightly extended the performance limits in ice. There was no discernable difference in lifeboat performance during transits through pack ice for different hull forms. Results from these model experiments were compared to predictions of hull resistance that were generated using the discrete element code DECICE3D by Lau and Simões Ré (2006). The numerical model underestimated the resistance in some cases as it does not consider hull deformation during ice loading and local ice crushing events. Additional model tests were conducted

in combinations of pack ice and waves for all three hull forms that were reported by Barker et al. (2004) and Sudom et al. (2006). The results indicated that the presence of waves in combination with pack ice can enhance the performance of a lifeboat by enabling travel through higher ice concentrations when waves were present. This was only the case when the vessel travelled with the waves. The vessels ability to transit pack ice in waves was found to depend mainly on the wave period and ice concentration, rather than on hull form (Sudom et al., 2006).

Igloliorte et al. (2007) reported full-scale field trials with a TEMPSC operating in ice during the winter of 2002. The craft was outfitted with a set of instrumentation to measure strain, hull deflection, heave, pitch and roll of the hull. In these un-powered field trials, the lifeboat was left un-manned in the ice and checked upon periodically via helicopter. The lifeboat hull was damaged due to ice pressure during the trials. Ice thickness was found to be a less important factor in lifeboat survivability than ice strength after observing the lifeboat extruded from the ice in various ice thicknesses. The paper described the development of a non-linear finite element model, using material properties developed from destructive testing of the TEMSPC that aimed to estimate the line loads on the hull and to investigate the role of the hull construction in the TEMPSC's ability to resist ice loading during pressure events (Igloliorte et al., 2007). Igloliorte et al. (2008) reported a second set of full-scale trials of a TEMPSC in broken and brash ice conditions in the spring of 2006. The approach was different from the previous trials as the lifeboat was manned and operated in ice conditions of concentration up to 9.5/10ths and in

thickness up to 35 cm. The TEMPSC demonstrated significant capability to operate in conditions which were managed by a supply vessel (Igloliorte et al., 2008).

A multi-year program of full-scale lifeboat trials were presented by Simões Ré et al. (2008), Kennedy et al. (2010), Simões Ré et al. (2011), Simões Ré and Veitch (2012, 2013), and Kennedy et al. (2014). Simões Ré et al. (2008) introduced the first set of trials conducted in May 2007, which investigated the performance of an instrumented 20-person conventional TEMPSC in open water, pack and level ice. Field trials results were well matched with model scale experiments. The results reported there are for a single lifeboat, so the effects of design parameters were not evaluated. A second set of trials was conducted in ice with the same lifeboat in April 2009. The lifeboat was fitted with a 6-component dynamometer and a bow shoulder impact panel to measure ice loads during impacts. The details of these trials were presented by Kennedy (2010). A semi-empirical model was developed based on Popov et al. (1968) to represent this type of craft interacting with ice and compared with the ice load data measured in these trials (Kennedy et al., 2010). The model was a modification of the earlier Popov model that considered hull deformation with an aim to make it applicable for predicting ice loads arising from composite structure vessels colliding with ice. The next field trials were done in March 2010 in pack ice conditions on a freshwater lake. Details of the field trials conducted from 2007 to 2010 were described by Simões Ré et al. (2011). Simões Ré and Veitch (2012) presented some ideas for improving the performance of lifeboat in terms of design and operational aspects based on the 2010 field trials. Transit (sail-away) distance and time were used as performance benchmarks and the effect of different ice conditions

(e.g. ice concentration, thickness, floe size) on performance was discussed in this paper. Simões Ré and Veitch (2012) identified the concentration of ice as one of the significant factors that limits the performance of lifeboat. The prospect of applying ice management was also mentioned. Coxswain's tactics and visibility lead to better performance of lifeboat maneuvering and it was suggested to improving the coxswain's visibility from a design point of view. Modification of the propulsion system and additional power made marginal improvement on the performance. From a structural point of view, the lifeboat hull was able to withstand the ice loading as no damage observed during the trials.

Simões Ré and Veitch (2013) focused on the local ice loads measured on the bow shoulder of the lifeboat hull during full-scale field trials in 2010. The performance limit of the lifeboat was discussed in terms of ice loads at different speed in different ice concentration. Results showed a weak relationship between measured maximum local loads and speed at impact. The study revealed that the fiberglass hull was adequate as the highest measured load was below the ultimate strength the fiberglass panel. Simões Ré and Veitch (2013) suggested measuring loads on the stem where the largest loads were likely to be experienced to get the complete history. That issue was addressed in 2013 and 2014 field trials. The lifeboat was outfitted with a bow appendage referred to as a "bow visor" (Kennedy et al., 2014). The bow visor was equipped with two load cells to measure the local ice loads on the lifeboat's stem. Kennedy et al. (2014) presented the results of measured stem loads in the 2013 field tests. Further analysis has been performed using the data sets captured during the 2013 and 2014 field trials and will be described in this thesis.

The UK Health and Safety Executive (2007) published a three phase research report that provided the structural design basis of TEMPSC in open water conditions. In the first phase, literature and data relevant to TEMPSC vessels and launch conditions were gathered and reviewed to form the basis for the structural design calculations to be performed in the subsequent phases of this project. The second phase identified a number of load events that are considered to be critical to the strength requirements of TEMPSC and maximum load capacities were estimated for each event. The final phase addressed the safety margins and the likelihood of each failure event was quantified. This study was exclusively intended to provide design requirements of lifeboats in open water and did not consider ice loading scenarios. The IMO (2007)'s International Convention for the Safety of Life at Sea (SOLAS) and corresponding International Life-Saving Appliance (2010) Code cover a wide range of issues for lifeboat regulations that includes construction, capacity, access, buoyancy, freeboard and stability, propulsion, fittings, equipment, markings, enclosure, capsizing and re-righting, protection against acceleration and protection against fire. Transport Canada (1992) released standards for lifeboats that govern the material selection, design, and construction of conventional lifeboats. These regulations and standards do not provide any guidance relevant to lifeboats in ice. The International Standards Organization (ISO) circulated a standard (ISO 19906, 2011) that includes a section regarding EER systems. This section defines the broad performance goals of EER systems, but does not offer any detailed design guidance related to the structural strength of lifeboat hulls during ice loading. Timco and Dickins (2005) proposed environmental guidelines for EER systems in ice-covered waters. The Canadian Coast Guard published Ice Navigation in Canadian Waters (2012), which was intended to

provide operational guidance for ice-going ships in all Canadian waters, including the Arctic, but does not include any guidelines for small craft in ice.

Suyuthi et al. (2012) studied some useful sources of classical statistical inference in relation to the ice induced loads on ship hulls. These procedures for statistical inference were also verified by numerical experiments. Ice loads measured on an offshore patrol vessel in full-scale field tests were analyzed with this statistical approach and it was found that the Weibull distribution model provided the best fit to the data. Li et al. (2006) developed an autoregressive model that establishes a relation between local pressure and global pressure. Frederking (2003) analyzed full-scale data measured on an icebreaker using a probabilistic approach to determine an annual probability of exceedance of ice pressures for a range of panel areas. Jordaan et al. (1993) introduced a method for analyzing local ice pressures on a probabilistic basis. An update to this method was proposed by Taylor et al. (2010), who used it to analyze the peak loads measured on icebreakers during collision with ice to provide guidance of design local pressures using probabilistic approach. This same approach is adapted here for analyzing the local ice loads measured on the lifeboat during the field trials that will be presented in this thesis.

3 Full Scale Experiments

3.1 Scope

This chapter describes the details of the 2013 and 2014 full-scale field experiments that were conducted with an instrumented Totally Enclosed Motor Propelled Survival Craft (TEMPSC) in varying pack ice conditions. The trials took place at Paddy's Pond (47°28'19.97"N, 52°52'58.74"W), which is located near St. John's, NL. The location of the trials site is shown in Figure 3.1. Data sets measured in these trials have been analyzed and the results are presented in this thesis.
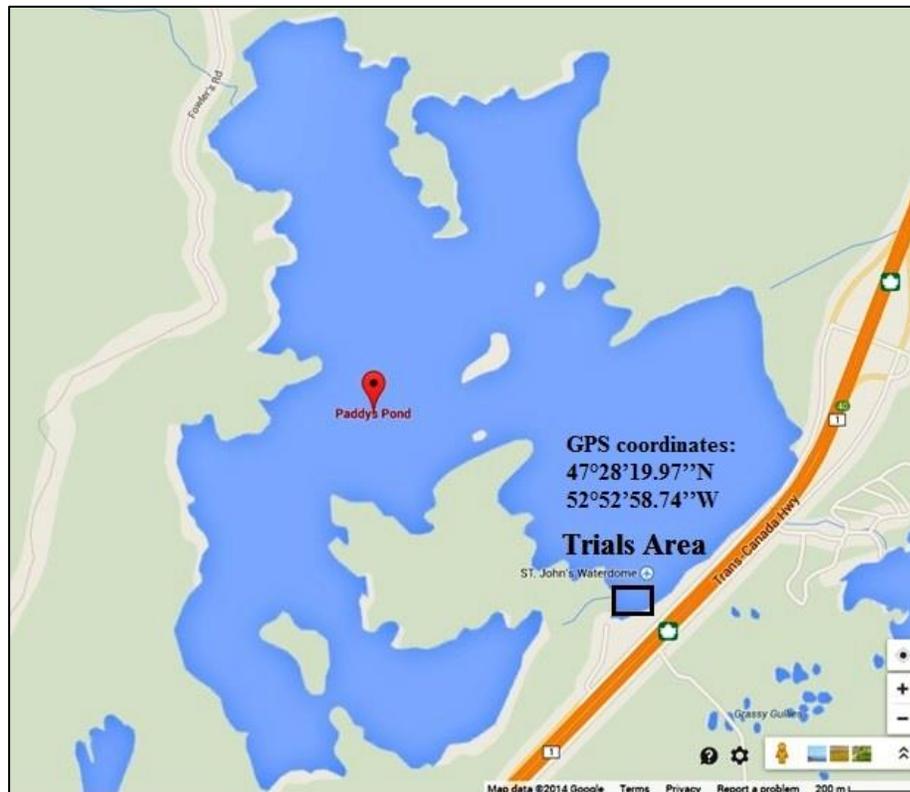
Figure 3.1: Paddy's Pond trials location

3.2   Lifeboat

The TEMPSC used in field trials has an overall length of 5.28 m, a maximum breadth of 2.20 m, a height of 2.70 m, and a moulded depth to the gunwale of 1.10 m. It was fabricated of glass-reinforced plastic with the hull, inner-hull, and canopy moulded as individual sections with poly-urethane foam as the buoyant material. It was built to the requirements prescribed by the SOLAS Convention (IMO, 1997) and the International Life-saving Appliance (LSA) Code (IMO, 2003). The lifeboat had a fully loaded displacement of 3665 kg, corresponding to 20 (75 kg) people. It was originally equipped with a 22 kW engine and a three bladed propeller inside a steerable nozzle. Modifications to the engine, propeller, and nozzle were made in 2009. Table 3.1 summarizes the details of the changes that were made with the lifeboat engine, propeller, and nozzle characteristics.

Table 3.1: TEMPSC engine, propeller and nozzle characteristics

TEMPSC powering, propeller, and nozzle	Original TEMPSC	Modified TEMPSC
Engine	22 kW	40 kW
Number of propeller blades	3	4, Kaplan
Propeller diameter / Propeller pitch	0.457 m / 0.279 m	0.457 m / 0.305 m
Nozzle inner / Outer diameter	0.50 m / 0.52 m	0.464 m / 0.556 m

3.3   Instrumentation

A 6-component dynamometer was fitted to the port side shoulder of the TEMPSC to measure the local ice loads on a 100 mm thick acrylic panel that was machined with the same curvature as the hull. A grid of 100 mm × 100 mm was marked on the acrylic panel.

The dynamometer consisted of 6 U2B force transducers. The three 50 kN load cells measured force across the beam of the lifeboat. Two of the 10 kN range load cells measured force along the length of the lifeboat and the other measured the vertical force. The total magnitude of loads measured in a horizontal plane during impacts is considered in the analysis. Figure 3.2 illustrates the installed port side shoulder panel and the arrangement of load cells within the load dynamometer. Further details of the lifeboat shoulder panel were described by Kennedy (2010).
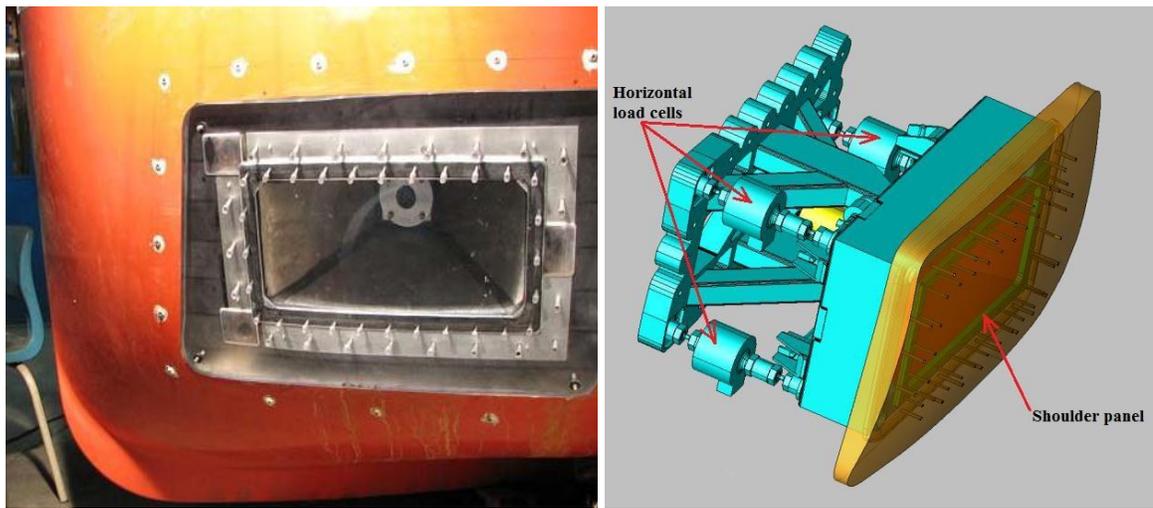
Figure 3.2: Installed shoulder panel and arrangement of load cells

The TEMPSC was also outfitted with a bow appendage, referred to as a "bow visor." The bow visor is mounted externally to the stem of the TEMPSC such that it effectively creates the TEMPSC's rake and entrance angles. The central component of the bow visor can be adjusted to different rake angles ranging from 5 to 20 degrees, while the panels of the bow visor can be adjusted to change the entrance angle from 50 to 90 degrees. The

bow visor was equipped with two load cells to measure the ice loads directed normal to the lifeboat's stem. The stem load is taken as the sum of loads measured by both of the loads cells during ice impacts. More details about the bow visor were discussed by Kennedy et al. (2014). Figure 3.3 shows the locations of the shoulder panel and bow visor on the TEMPSC.

Figure 3.3: Position of shoulder panel and bow visor of the TEMPSC

The lifeboat also contains a suite of other instrumentation to allow measurement of different parameters during testing. The other lifeboat instrumentation is summarized in Table 3.2. Further details of the instrumentation package were described in a report by Simões Ré et al. (2012).

Table 3.2: TEMPSC instrumentation package

Instrument	Description
Remote control system	This feature was added to the lifeboat so that the lifeboat could be driven externally using remote control. The remote control system was used for a sub-set of tests.
Differential Global Positioning System (DGPS)	latitude, longitude and time measures
Roll and pitch sensors	Measures roll and pitch independently.
Yo-Yo potentiometer and tachometer	Measures rudder angle and shaft speed.
Anemometer	Measures wind speed and direction
Linear Variable Differential Transformer (LVDT)	Measures the displacement of the live dynamometer mounting frame and the relative displacement between the sea-chests.
Video cameras	A total of six cameras were installed with the lifeboat to get a complete view of its surroundings, the local ice conditions and the ice impacts.

3.4   Data Acquisition System

The instrumentation was connected to the TEMPSC Data Acquisition System (DAS), sampling data at low, medium, and high speed. The high speed DAS was a 3031 USB Daqboard. The medium and low speed DAS were Programmable Interface Controllers (PIC). A video acquisition system was also used. All data was recorded to a laptop computer that is secured within the TEMPSC. This computer can be accessed at an on-shore site through wireless connection, so that the data can be started and stopped external to the TEMPSC. The acquired data was post-calibrated by a separate calibration program and transferred to the main computer. Subsequently, all the calibrated data was

imported into the program IGOR for analysis. Further details of the DAS and calibration of data have been described previously by Simões Ré et al. (2012).

3.5   Field Trials 2013

The 2013 lifeboat trials were conducted in Paddy's Pond during March, 2013. The purpose of these field trials was to assess both structural and operational performance of the modified TEMPSC in various pack ice conditions. The particulars of the ice field, test plan, and the data resulting from the 2013 field tests are described in the following sections. A fuller description of the 2013 ice trials is presented in a report by Kennedy et al. (2014).

3.5.1   Description of Ice Field

The ice field was manually cut from a level ice sheet that was 86 m long and 38 m wide. Ice floes were cut from this level ice cover to an average size of 3 m long by 3 m wide. The average measured ice thickness was 38 cm. The ice field dimensions were selected to be representative of an icebreaker channel, through which a TEMPSC could be expected to navigate. An open water region was created at the entrance of the ice field and was used as the TEMPSC preparation area for ice testing. Figure 3.4 includes a photograph of the ice field and a schematic that displays the layout of the ice field.

Figure 3.4: Prepared ice field for lifeboat trials

A series of tests was conducted at ice concentrations ranging from 9/10ths to 4/10ths. To reduce the ice concentration, selected ice floes were removed from the ice field by manually pushing them into the open water preparation area. The ice floes were individually lifted out of the water using an excavator. Figure 3.5 illustrates the removal process of a single ice floe and highlights the average thickness of each floe.

Figure 3.5: Ice floe removal using an excavator

The ice floes were composed of a solid ice layer topped with a layer of compressed snow. The mass of an individual ice floe was approximately equal to the mass of the TEMPSC. Overnight, the temperature dropped significantly and the ice floes re-froze together forming a single ice sheet. These pieces were manually separated each morning before starting the tests to maintain a consistent piece size.

The environmental conditions in the field, such as wind speed, wind direction, air temperature and relative humidity, were recorded during the test program. The range of each of these parameters, throughout the test period, is summarized in Table 3.3. The environmental conditions during a given test may influence the performance of the TEMPSC. For example, the temperature may affect the strength of ice and wind speed and direction may affect the TEMPSC's operational performance, in terms of distance and speed travelled, in a given ice condition.

Table 3.3: Environmental conditions (2013 testing)

Environmental parameter	Range in values
Wind gust speed (km/h)	0 to 80
Wind direction	NE to NW
Temperature (^{o}C)	-17 to +10
Relative humidity (%)	40 - 100

3.5.2   Test Plan

There were a total of 94 tests conducted at different ice concentrations during the 8-day test program. Some tests were conducted during night, in limited light levels. The test

variables, described in Table 3.4, included ice concentration, visibility level, type of operation, and coxswain.

Table 3.4: Test variables

Test variables	Description
Ice concentration	9/10ths to 4/10ths. It relates to the percentage of the ice field area that has ice.
Visibility level	I. Day or night. Few tests were conducted at night in limited visibility. II. TEMPSC hatch position, either open or closed. The coxswain had better visibility when the hatch was open and his/her head was out of the canopy.
Coxswain	There were eight coxswains.
Type of operation	Onboard driver or remote operation.

The purpose of a single test was for the TEMPSC to maneuver as far as possible towards the opposite end of the ice field, in a timely manner. The test was ended when either the TEMPSC could no longer make any forward progress through the ice field over a five minute period or when it successfully reached the other end of the field.

3.5.3   Description of Data

During 2013 field trials, local ice loads and MotionPak linear acceleration and angular rate data were sampled at a frequency of 4000 Hz. A data analysis procedure was developed to calibrate the raw data and save the output as independent columns of data. Impact force and corresponding roll, pitch, propeller speed, TEMPSC speed, and rudder angle at the time of impact were measured both at the bow shoulder panel and bow visor panel during each test. The total impact force on the bow shoulder was found by adding

of the measurements from the three load cells oriented normal to the shoulder panel and then adjusting this sum by subtracting the tare value (the measured load reading when no ice load was applied). To compute the total bow visor load, the loads measured by each of the two load cells housed within the bow visor system were added and then adjusted using the corresponding tare value. A minimum threshold value of 4 kN was set and only ice loads higher than this value were considered in the analysis. Table 3.5 represents a sub-set of the data acquired from a single test in 8/10ths ice concentration.

Table 3.5: Data summary of a single test

Time (sec)	Bow shoulder load (kN)	Roll (deg)	Pitch (deg)	Propeller rpm	TEMPSC speed (knots)	Rudder angle (deg)
184	10.1	2.4	0.2	641.4	2.0	13.3
190	6.0	0.1	2.8	636.6	1.4	16.1
191	8.4	0.1	2.8	631.1	1.3	16.3
261	4.6	2.4	3.1	795.2	0.8	12.2
262	5.0	0.5	3.2	825.1	0.8	12.3
268	15.2	11.3	4.3	977.8	0.7	0.5
308	14.5	0.6	0.9	861.6	0.2	12.9
453	10.5	1.5	3.4	588.6	0.6	9.2
523	4.2	6.1	4.3	982.4	0.6	6.2
577	6.1	0.2	0.7	629.7	1.0	7.0
658	4.5	0.4	2.8	625.2	1.0	11.7
666	6.6	4.8	1.4	949.7	1.3	16.3
724	4.9	7.6	3.8	815.2	0.3	5.2
740	4.8	4.8	5.7	916.4	0.2	12.8
741	7.7	4.6	5.1	915.7	0.2	7.5
743	4.2	4.5	6.2	915.0	0.2	4.2
764	5.6	0.7	2.0	824.7	1.0	20.2
803	30.3	1.9	0.7	569.5	0.0	30.0

For each test, the ice loads were identified on a DGPS plot with the corresponding TEMPSC Course Over Ground (COG) trajectory that illustrates the position the peak loads occurred. These plots were used to compute the sail-away distance, path length, and mean speed of the lifeboat in each test. The sail-away distance represents the straight-line distance between two points. In Figure 3.6, it started when the TEMPSC entered the ice field and ended at the farthest point reached during the test. The path length is the actual distance travelled by the lifeboat, which may either be equal to or larger than the sail-away distance. The mean speed of a given test is defined as the sail-away distance divided by the total time required for the lifeboat to travel this distance.

A DGPS plot of a test in 8/10ths ice concentration is shown in Figure 3.6. Peak loads above 4kN measured on the bow shoulder are identified on the trajectory of the lifeboat. Sail-away distance, lifeboat path and the perimeter of ice field are also illustrated. The time series data indicating bow shoulder impact loads and corresponding TEMPSC speed for this test is shown are Figure 3.7. Each load peak in the load trace that exceeded the 4 kN threshold was considered as a single event. A total of 2260 impact events were measured from 94 tests, of which 1725 were recorded at the bow visor and 535 were recorded at the bow shoulder.
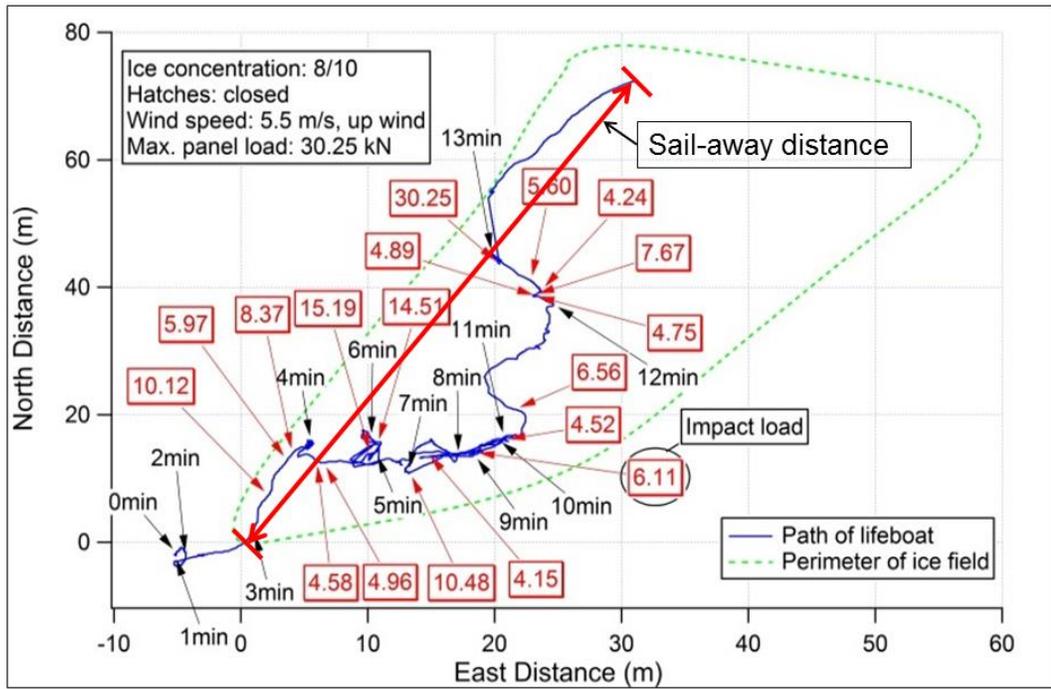
Figure 3.6: DGPS plot illustrating impact loads at bow shoulder and sail-away distance
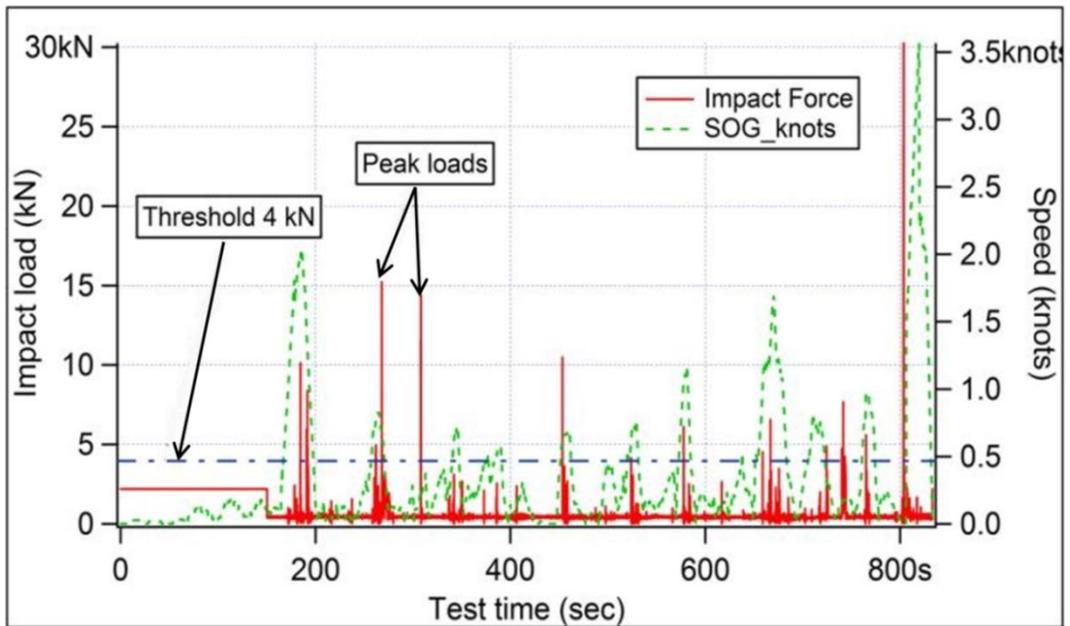
Figure 3.7: Impact loads at bow shoulder and speed of the same test

3.6   Field Trials 2014

The 2014 field trials were conducted during March, 2014 in controlled pack ice conditions. The location of these tests was the same as the location of 2013 field testing. Data collected during the 2014 field trials represents more severe ice conditions than previous trials and can provide insight as to how the TEMPSC performs in these conditions. Details of the ice field, test plan, and measured data from the 2014 trials are provided in the following sections. A fuller description of the 2014 ice trials is presented by Kennedy et al. (2014).

3.6.1   Description of Ice Field

The test site was cut from level ice cover that was approximately 80 m long and 35 m wide. Each ice block was cut to be approximately 3 m × 3 m. An average thickness of 0.51 m was measured. The average ice piece mass, 4590 kg, is approximately equal to 1.25 times the mass of the full-loaded TEMPSC. The ice floes were manually managed by the trials team during the tests, consistent with the 2013 field trials methods. Figure 3.8 illustrates the ice field during the 2014 field trials.

Figure 3.8: Ice field and individual ice piece

The ice floes were composed of a bottom layer of solid ice topped with a layer of compressed snow. Wind speed, temperature, and precipitation at the test site were recorded during the program. The range of each of these parameters, throughout the test period, is summarized in Table 3.6.

Table 3.6: Environmental conditions (2014 trials)

Environmental parameter	Range in values
Wind gust speed (km/h)	0 to 80
Temperature (^{o}C)	-17 to +11
Total precipitation (mm)	0 – 10.5

3.6.2 Test Plan

There were a total of 48 tests conducted in ice concentrations ranging from 9/10ths to 5/10ths during the 5-day test program. The test variables were similar to those presented in Table 3.4. The TEMPSC was operated by two different coxswains: one experienced in navigating the TEMPSC through ice and another one with less familiarity with the TEMPSC and ice operations. Other parameters of the test plan included the bow visor configuration and the type of test. A few tests were completed without side panels on the bow visor. The bow visor rake angle was fixed to 20 degree for all the tests. There were a sub-set of 8 tests conducted in which the TEMPSC navigated at set propeller speed values, towards an individual ice block and then impacted the ice block at the stem. These straight-line, relatively high speed impacts generated higher ice loads than the ice loads measured during the other testing. The 2014 field trials test plan is summarized in Table 3.7.

Table 3.7: 2014 ice field trials test plan (Kennedy et al. 2014)

Ice concentration	No. of tests	Test details	Rake angle	Entrance angle
0	1 to 2	Bollard tests - No bow visor panels	20	NA
0	1 to 2	Inclining tests - No bow visor panels	20	NA
0	1 to 2	Roll decay tests - No bow visor panels	20	NA
0	1 to 2	Push on bow visor with ice edge - No bow visor panels	20	NA
9	5 to 10	Tests in 9 tenths ice concentration - No bow visor panels	20	NA
8	5 to 10	Tests in 8 tenths ice concentration - No bow visor panels	20	NA
8	5 to 10	Tests in 8 tenths ice concentration -with bow visor panels	20	50
8	5 to 10	Tests in 8 tenths ice concentration –with bow visor panels - NIGHT	20	50
7	5 to 10	Tests in 7 tenths ice concentration - with bow visor panels	20	50
6	5 to 10	Tests in 6 tenths ice concentration - with bow visor panels	20	50
5	5 to 10	Tests in 5 tenths ice concentration - with bow visor panels	20	50
0	2 to 5	Speed Tests - Tests in which TEMPSC travels through open water to get up to speed and then impacts a single piece of ice (not level ice edge). Ice piece mass $= 1.0 \times$ TEMPSC mass	20	50
0	2 to 5	Speed Tests - Tests in which TEMPSC travels through open water to get up to speed and then impacts a single piece of ice (not level ice edge). Ice piece mass $= 1.25 \times$ TEMPSC mass	20	50

3.6.3   Description of Data

The 2014 field test data was analyzed using the same procedure that was described in section 3.5.3. A minimum threshold value was set to 4 kN, which was consistent with 2013 trials data analysis. The data set consists of a total of 2433 impact events, of which 1875 were recorded at the stem and 558 were recorded at the bow shoulder.

4 Probabilistic Analysis of Ice Loads

4.1 Scope

This chapter presents an analysis of local ice loads using probabilistic approach. For operational ice load models, emphasis is on the mean behavior, and so ensemble data are used in the analysis to model the overall distribution. For design ice loads, focus is on the extreme values of ice pressure and the event-maximum method has been used.

4.2 Operational Ice Loads

4.2.1 Methodology

Ice load data was categorized according to three different levels of ice concentration. Ice concentrations from 8/10ths to 9/10ths were defined as high ice concentration (C_H). The next two levels, 6/10ths and 7/10ths, were labeled as medium (C_M), and ice concentrations of 5/10ths and 4/10ths were defined as low ice concentration (C_L). No test was performed at 4/10ths ice concentration during 2014 field trials. Therefore, only the ice load data measured at 5/10ths ice concentration was defined as low ice concentration for 2014 field tests. Histograms of impact loads for the stem and bow shoulder were generated to investigate the probability distribution for each of the ice concentration levels.

4.2.2   2013 Ice Load Data

4.2.2.1 Ice Load Distributions for Stem

During each test, the TEMPSC progressed through a defined ice concentration and made a series of impacts with ice. The vessel's speed was variable, largely dependent on how it was operated by the coxswain. The overall distribution of 2013 stem load data for all tests is shown in Figure 4.1.
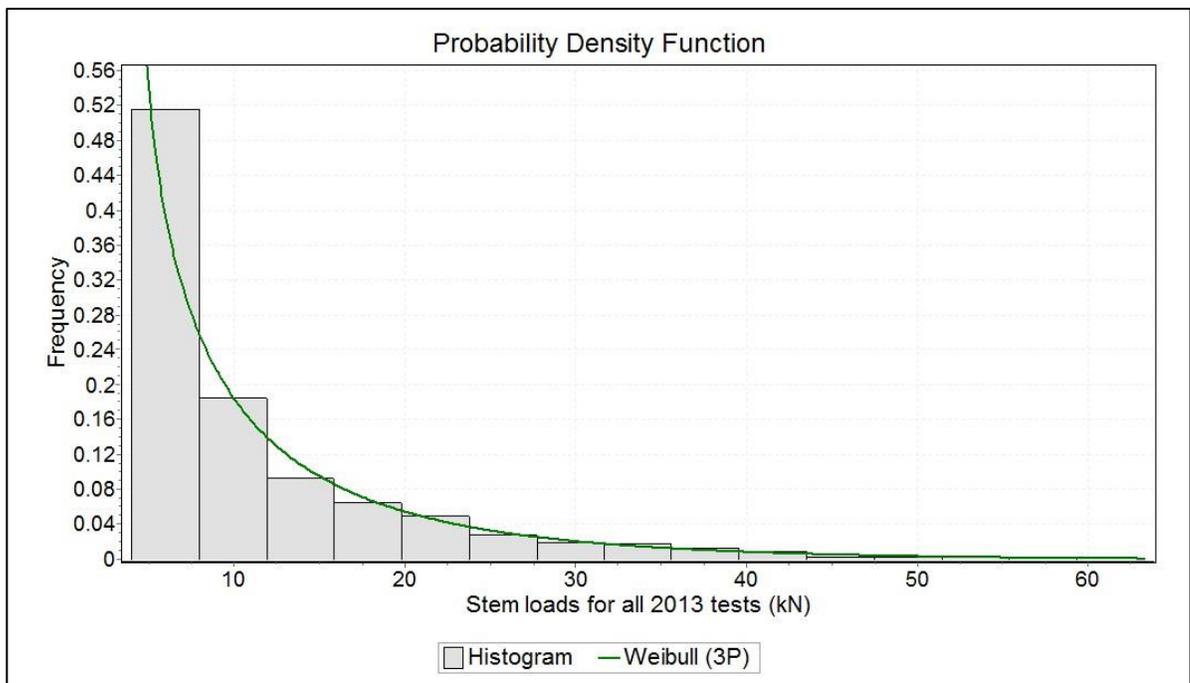
Figure 4.1: Histogram of stem loads for all 2013 tests

Histograms for the high, medium, and low ice concentration cases are shown in Figure 4.2, Figure 4.3, and Figure 4.4, respectively. The frequency of low magnitude impact loads is high and decreases exponentially. Impact loads on the stem are well fitted with a Weibull distribution in each category. More than 50% of all stem load events are lower

than 8 kN. The largest load values on the horizontal coordinate of each histogram slightly decreases with decreasing ice concentration. The maximum ice load measured on the bow visor was 63.3 kN at high ice concentration, 57.4 kN at medium ice concentration, and 51.5 kN at low ice concentration level, respectively.
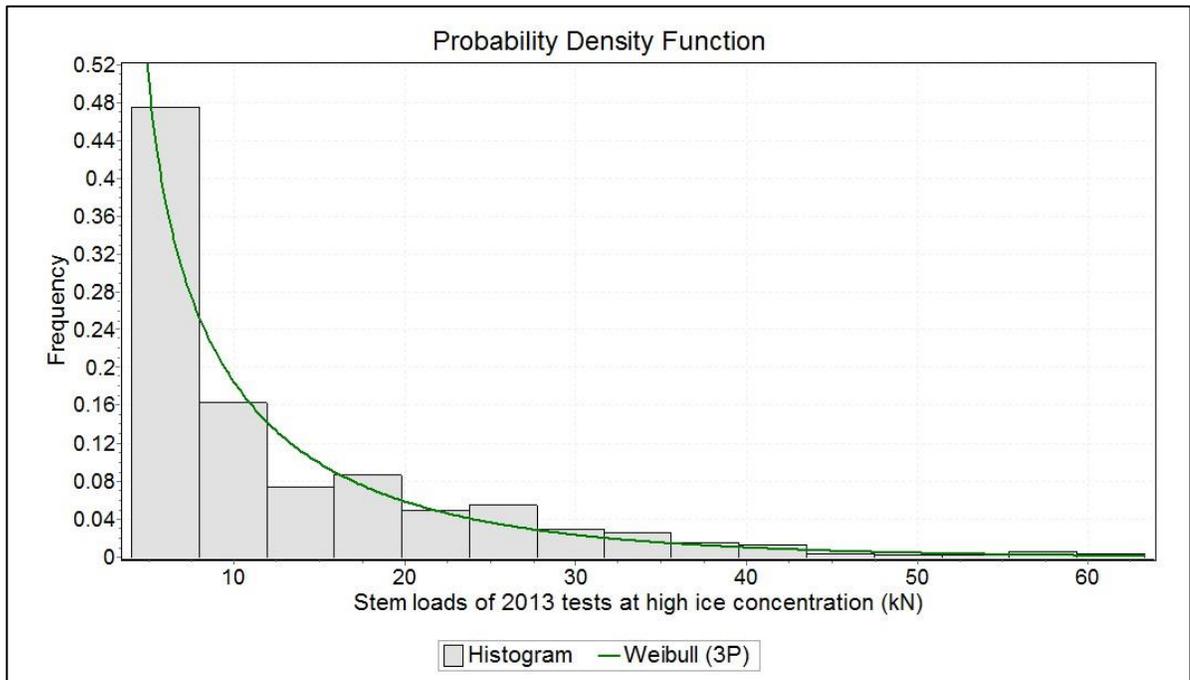
Figure 4.2: Histogram of stem loads of 2013 tests at high ice concentration
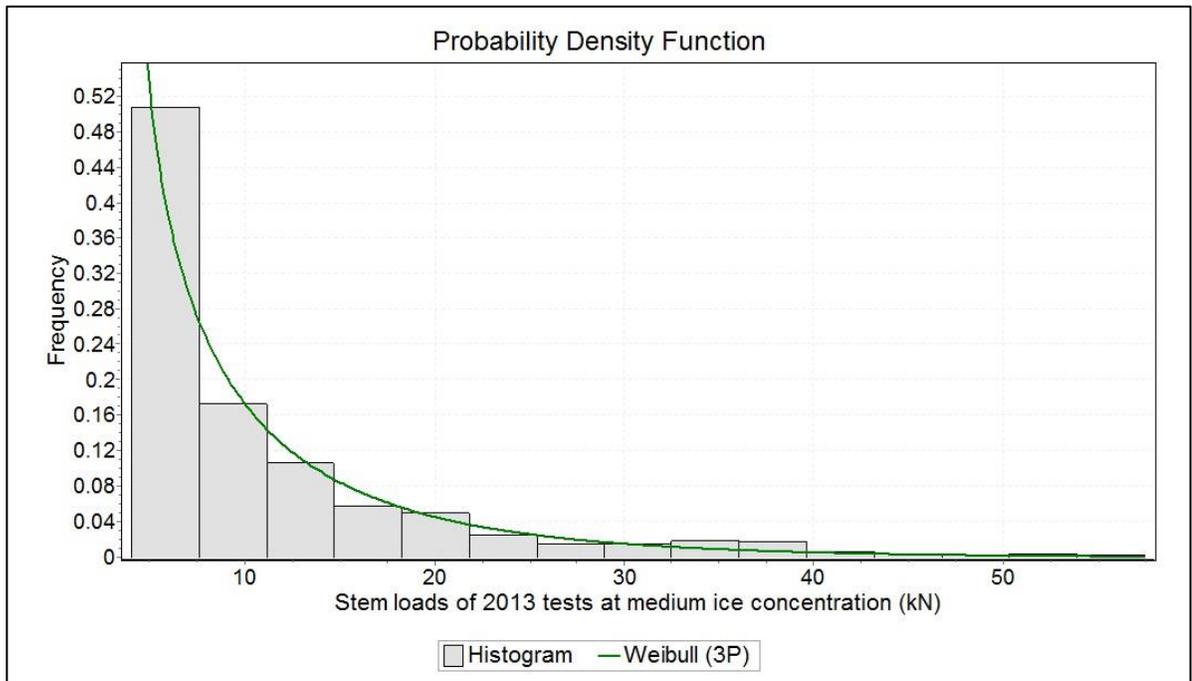
Figure 4.3: Histogram of stem loads of 2013 tests at medium ice concentration
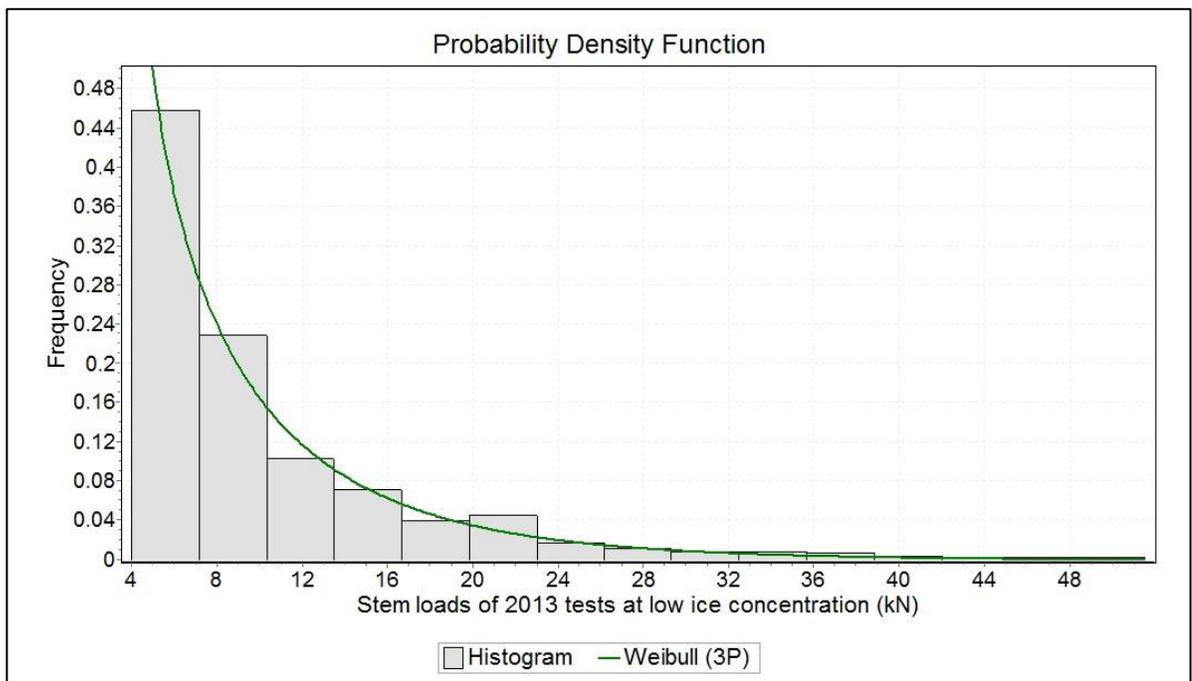
Figure 4.4: Histogram of stem loads of 2013 tests at low ice concentration

4.2.2.2 Ice Load Distributions for Bow Shoulder

Figure 4.5, Figure 4.6, Figure 4.7, and Figure 4.8 illustrate the 2013 bow shoulder load histograms for all tests, high, medium, and low ice concentration cases, respectively. Again, the Weibull distribution provides a reasonable fit for all ice concentration categories. The maximum range of measured ice loads is significantly lower on the bow shoulder area than on the stem. The maximum load measured on the bow shoulder was 34.3 kN during a test in a medium ice concentration level.
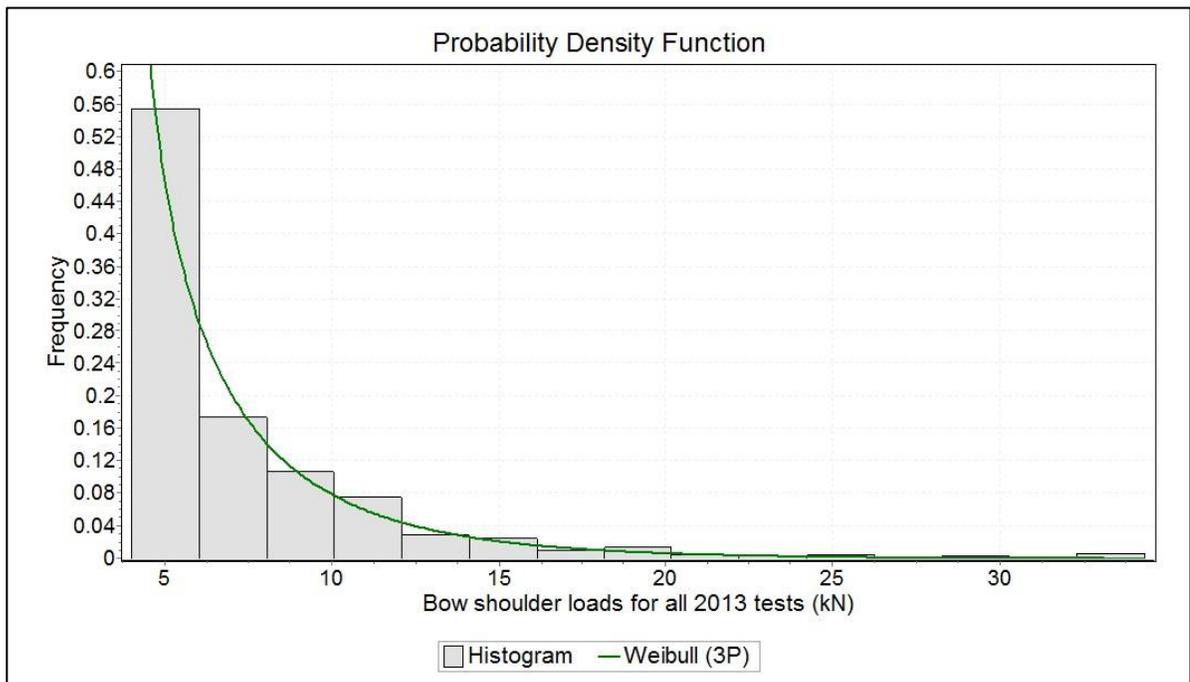
Figure 4.5: Histogram of bow shoulder loads for all 2013 tests
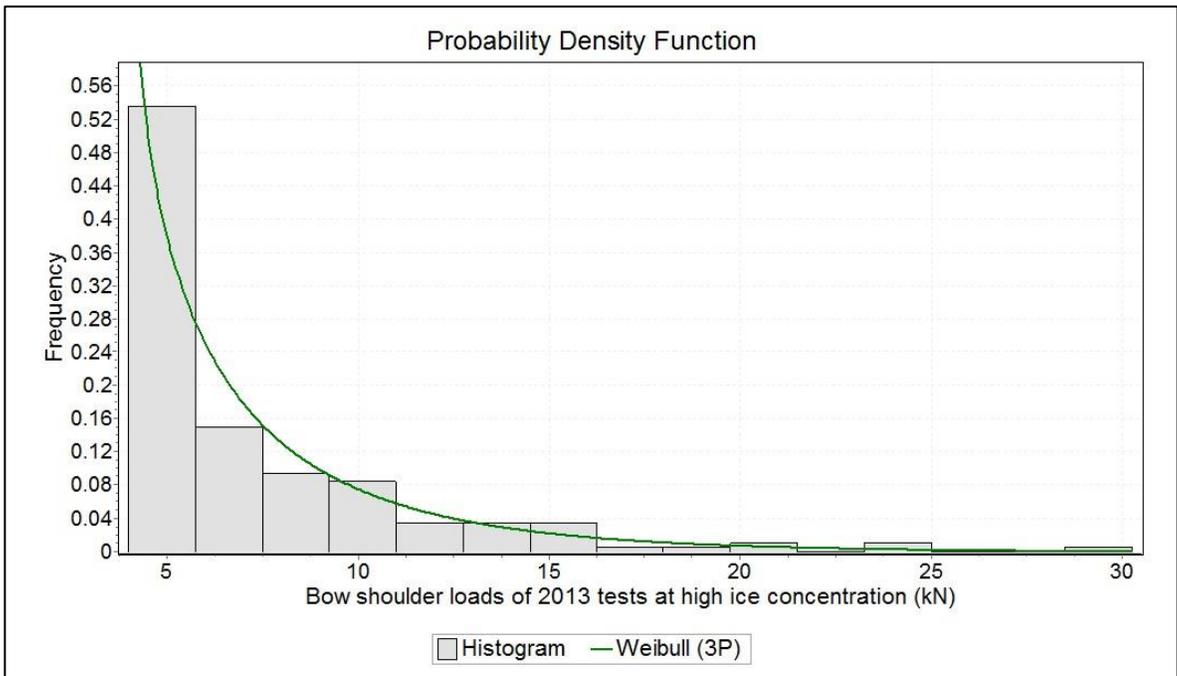
Figure 4.6: Histogram of bow shoulder loads of 2013 tests at high ice concentration
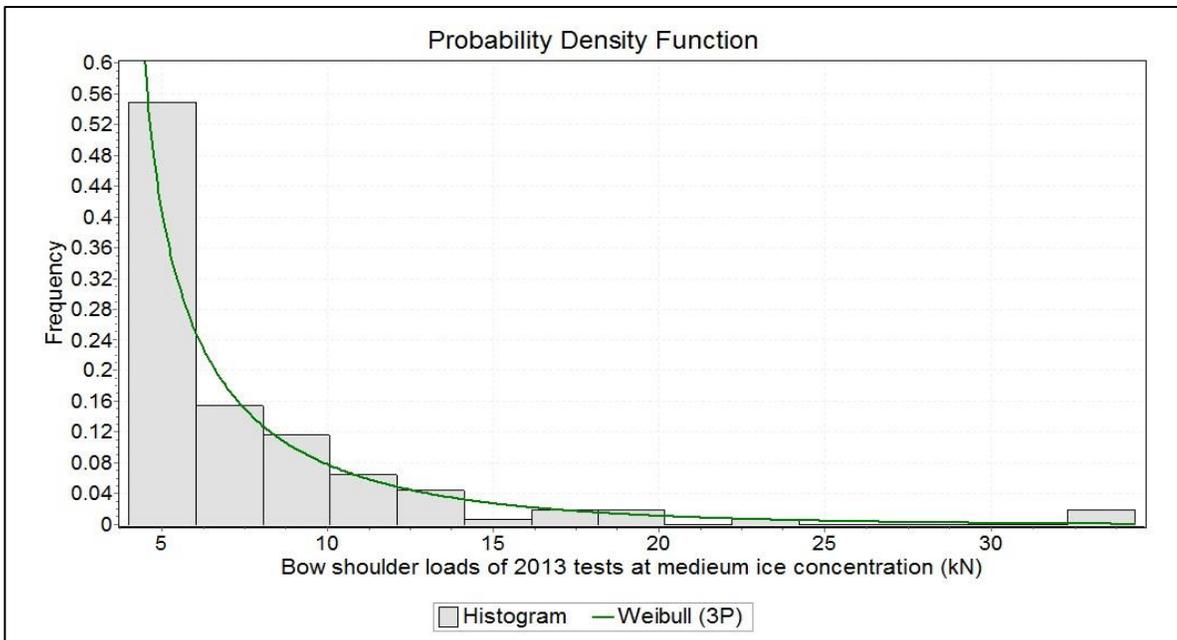
Figure 4.7: Histogram of bow shoulder loads of 2013 tests at medium ice concentration
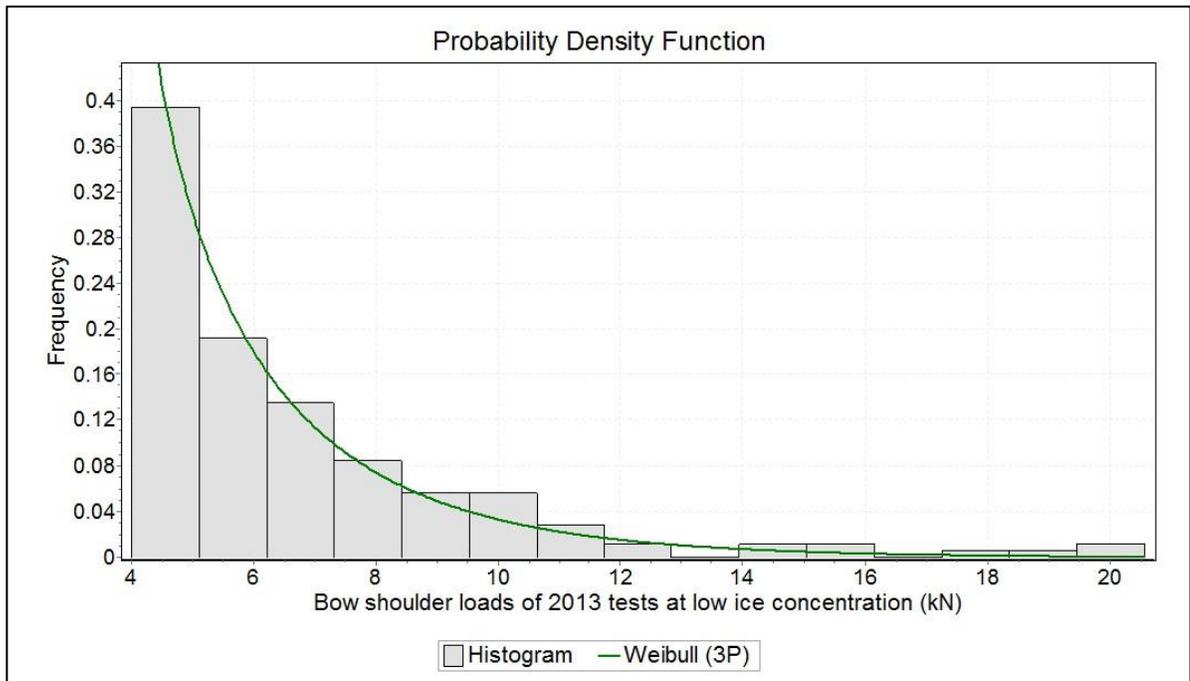
Figure 4.8: Histogram of bow shoulder loads of 2013 tests at low ice concentration

4.2.3 2014 Ice Load Data

4.2.3.1 Ice Load Distributions for Stem

The overall distribution of 2014 stem load data for all tests is shown in Figure 4.9. In the lower range, this distribution is generally consistent with the 2013 stem loads distribution as 43% of measured loads were below 8 kN during 2014 field trials. The maximum range of impact loads is higher in the 2014 tests as is clearly seen from the histogram. Several loads measured during the 2014 tests had magnitudes higher than 63.3 kN (the highest load measured in 2013 tests). The maximum 2014 load was 117.9 kN. Similar operating conditions as the 2013 field test were maintained during 2014 field tests, except the use of ice floes having higher average ice thickness (i.e. greater mass). The lifeboat experienced

higher magnitude of impact loads while it was progressing through the ice floes of higher

mass than the previous year tests.
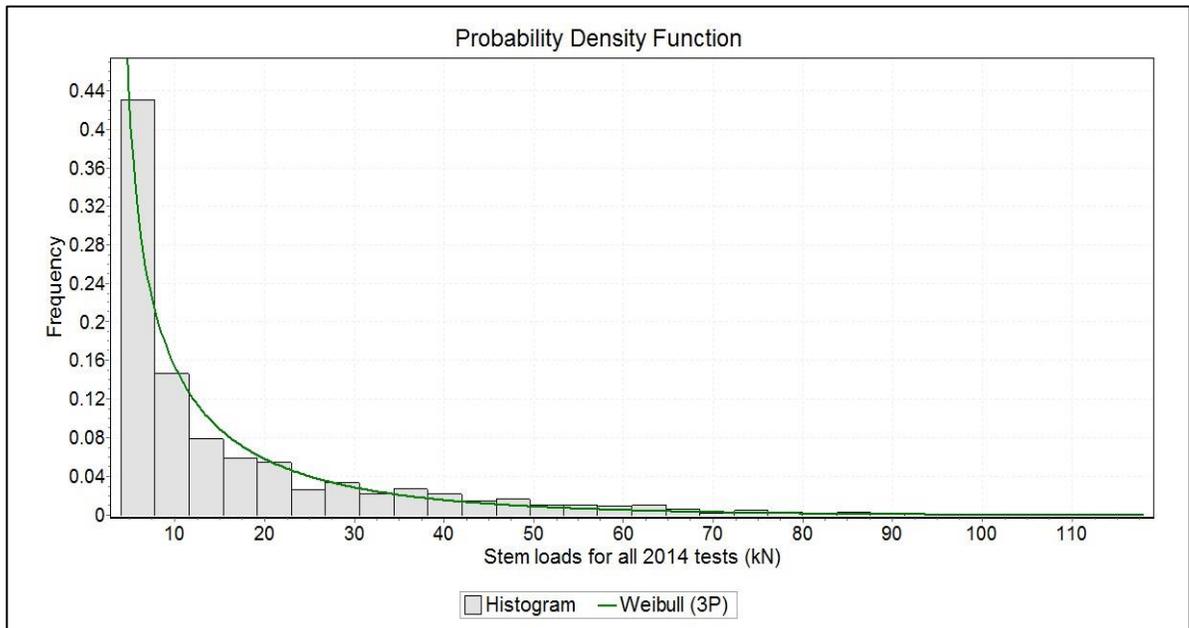
Figure 4.9: Histogram of stem loads for all 2014 tests

Histograms for the high, medium, and low ice concentration cases are shown in Figure

4.10, Figure 4.11, and Figure 4.12, respectively. The largest load values on the abscissa of

each histogram decreases slightly with decreasing ice concentration, as was the case for

the 2013 stem load data.
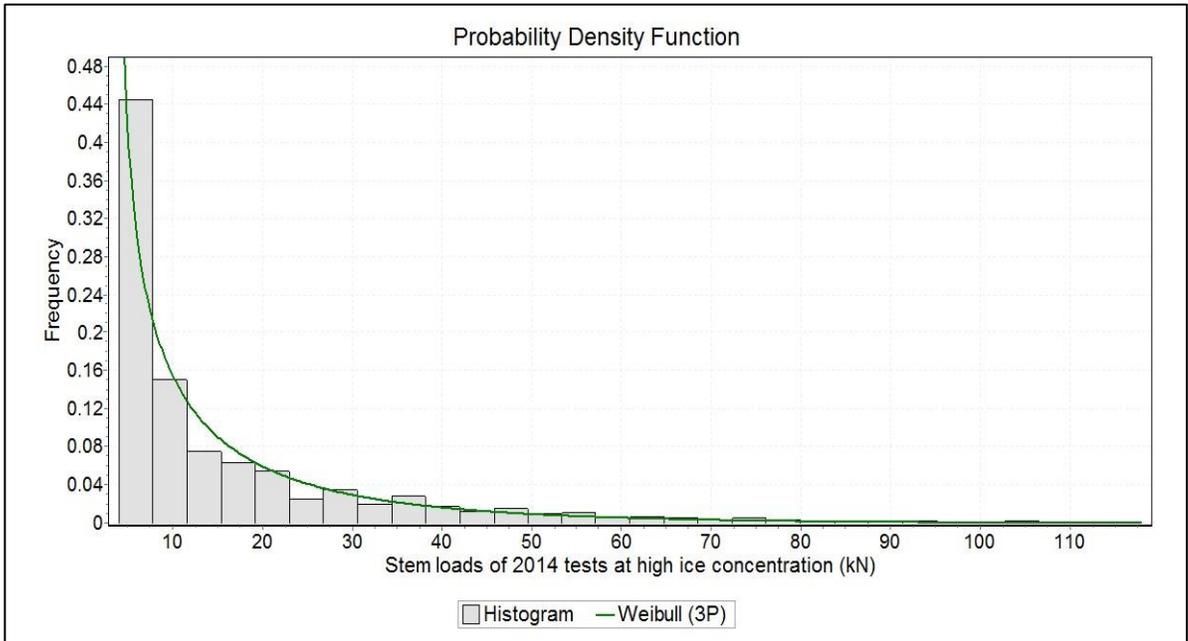
Figure 4.10: Histogram of stem loads of 2014 tests at high ice concentration
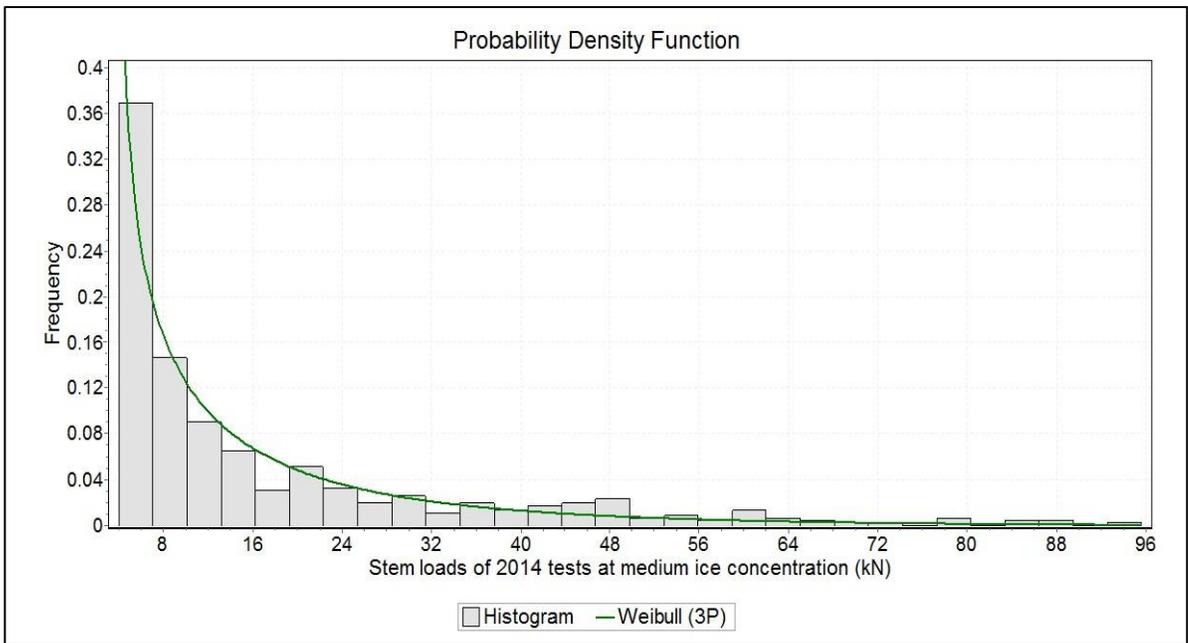

**Figure 4.11: Histogram of stem loads of 2014 tests at medium ice concentration**
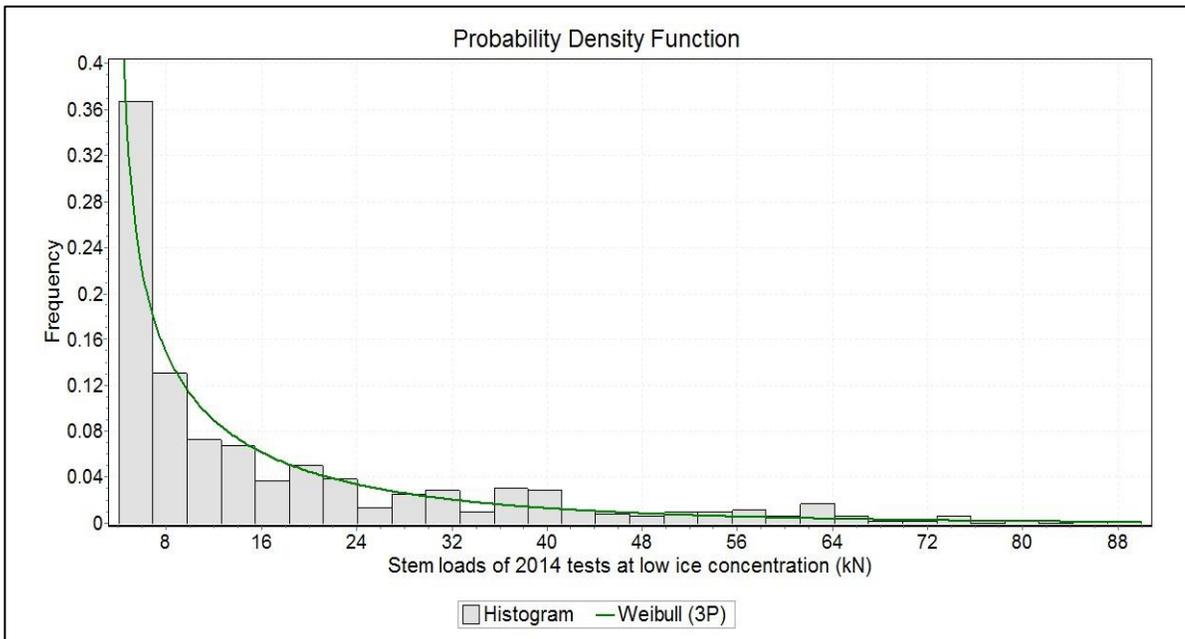
Figure 4.12: Histogram of stem loads of 2014 tests at low ice concentration

4.2.3.2 Ice Load Distributions for Bow Shoulder

Figure 4.13, Figure 4.14, Figure 4.15, and Figure 4.16 illustrate the 2014 bow shoulder load histograms for all tests, high, medium, and low ice concentration cases, respectively. The Weibull distributions are fitted for all ice concentration categories. The maximum range of measured ice loads is significantly lower on the bow shoulder area than on the stem. The maximum load measured on the bow shoulder was 62.7 kN, which is close to the highest load (63.3 kN) measured on the stem during 2013 field tests.
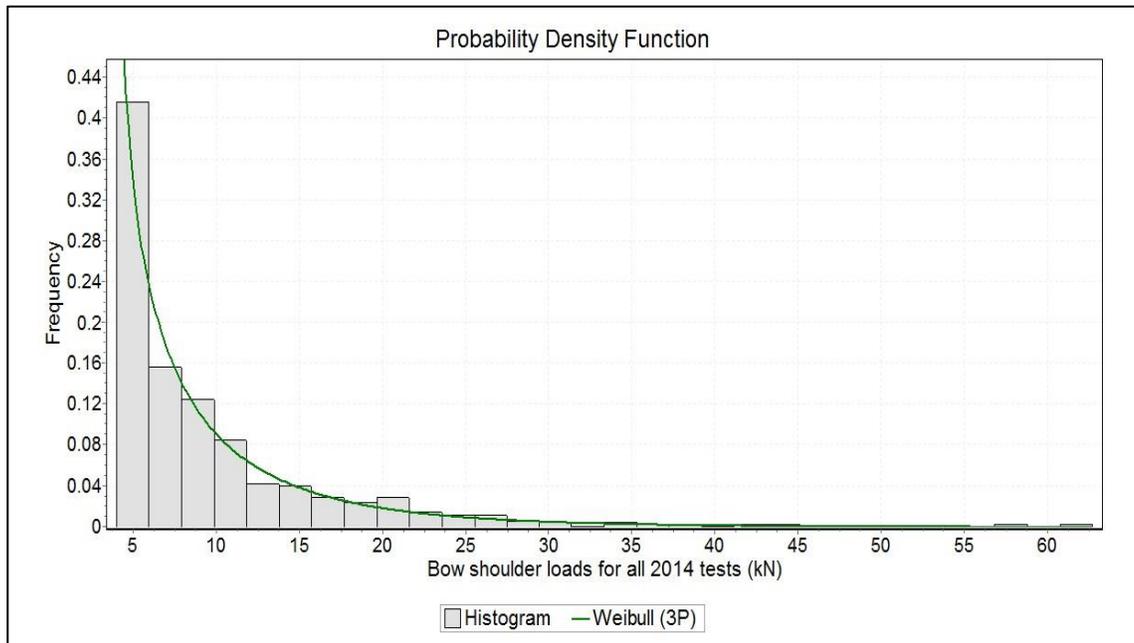
Figure 4.13: Histogram of bow shoulder loads for all 2014 tests
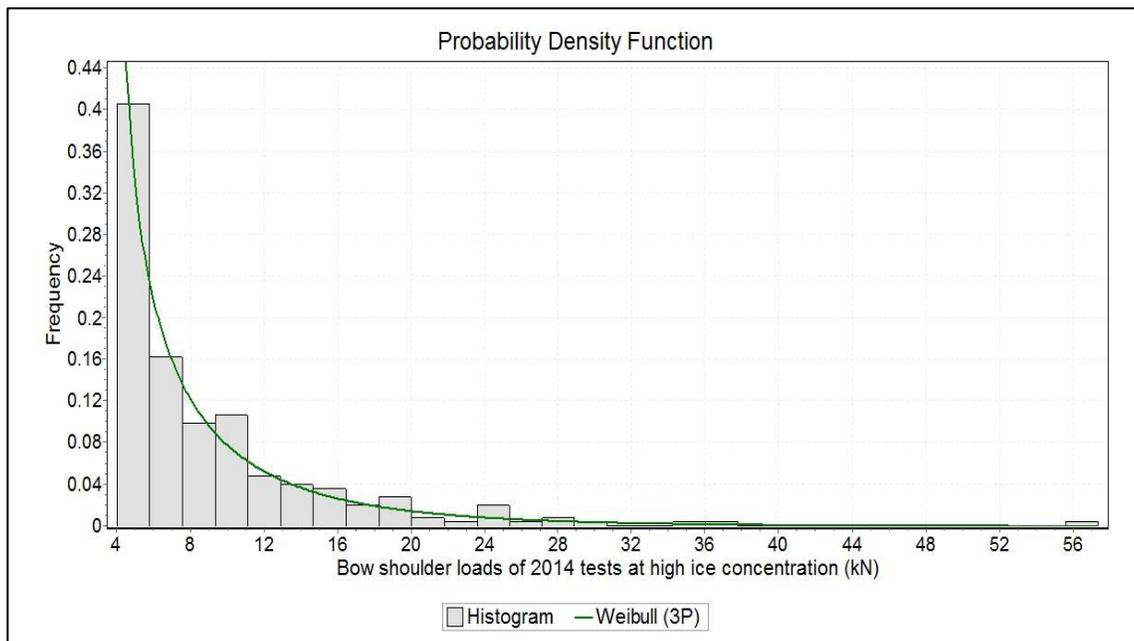

Figure 4.14: Histogram of bow shoulder loads of 2014 tests at high ice concentration
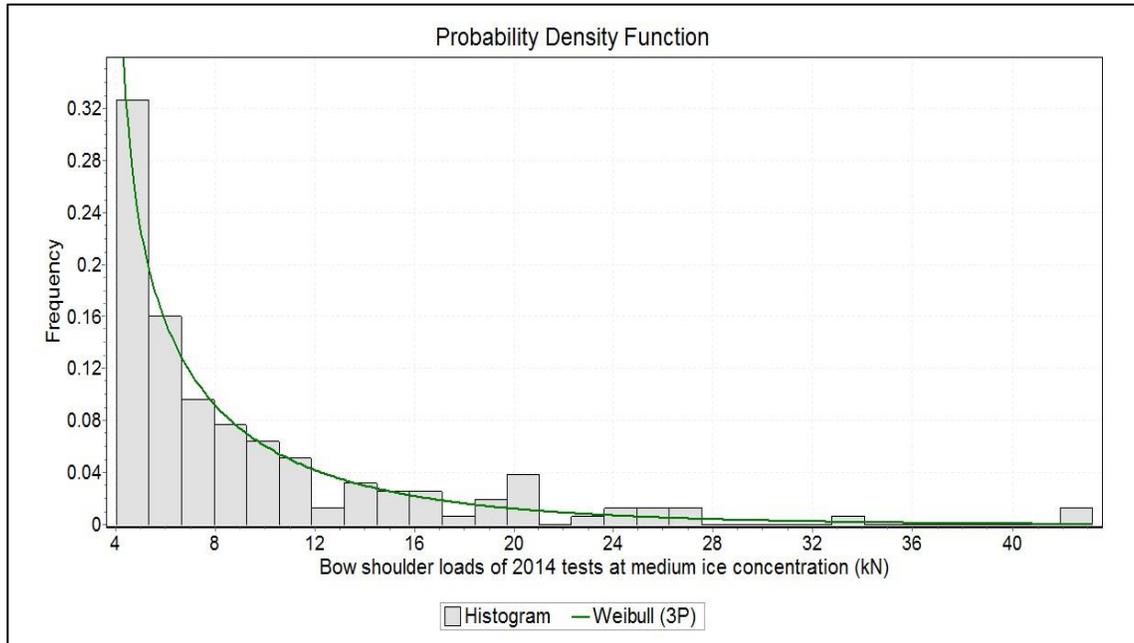
**Figure 4.15: Histogram of bow shoulder loads of 2014 tests at medium ice concentration**
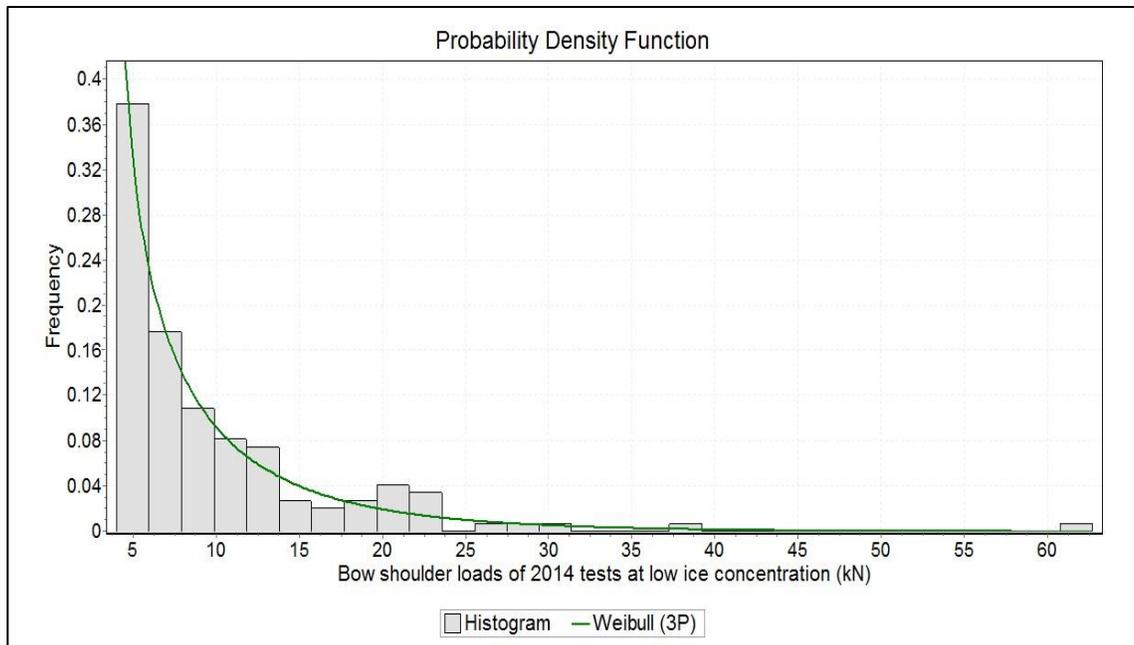
Figure 4.16: Histogram of bow shoulder loads of 2014 tests at low ice concentration

4.2.4   Summary of Distribution Parameters for Operational Ice Loads

Table 4.1 summarizes the Weibull parameters for 2013 ice load data, which is presented in section 4.2.2. The change of scale parameter is insignificant. The shape parameter value decreases from high to low concentration levels for both load panels. These values are higher for the stem load cases than the bow shoulder load cases.

Table 4.1: Weibull parameters for 2013 ice load data

Ice concentration	Stem loads 2013		Bow shoulder loads 2013	
	Weibull scale parameter, η	Weibull shape parameter, β	Weibull scale parameter, η	Weibull shape parameter, β
C_H	0.78	7.90	0.83	3.17
C_M	0.79	6.34	0.71	3.16
C_L	0.85	5.52	0.89	2.12
All 2013 load data	0.77	7.12	0.81	2.76

Table 4.2 summarizes the Weibull parameters for 2014 ice load data, which is presented in section 4.2.3. The shape parameter values are higher for 2014 data than the 2013 data for both load panels.

Table 4.2: Weibull parameters for 2014 ice load data

Ice Concentration	Stem Loads 2014		Bow shoulder Loads 2014	
	Weibull scale parameter, η	Weibull shape parameter, β	Weibull scale parameter, η	Weibull shape parameter, β
C_H	0.72	10.63	0.75	4.07
C_M	0.73	10.69	0.77	4.70
C_L	0.71	11.64	0.78	4.92
All 2014 load data	0.71	10.32	0.78	4.66

4.3 Local Design Ice Pressure

4.3.1 Methodology

According to the event-maximum method, the peak pressures calculated from the measured loads were ranked in descending order on a given area for high, medium, and low ice concentration and plotted against the natural logarithm of the plotting position (P_e). The Weibull plotting position was used for simplicity, given as *[i / (j+1)]*, where i is the rank of the individual data points from a set of *j* pressures (Jordaan et al., 1993; Taylor et al., 2010). A best-fit line was fitted to the tail (top 20% peak pressures) of each distribution, which was assumed to follow an exponential distribution, to give:

$$F_x(x) = 1 - exp(- (x - x_0)/\alpha) \tag{4.1}$$

where x_0 and α are constants for a given area, and x is a random quantity denoting pressure. The parameter α is the inverse slope of the best-fit line, and x_0 is the intercept of this line with the abscissa. In addition, the parameter α is a function of the area, represented by the curve $\alpha = Ca^D$, where *a* is the local area of interest, and *C* and *D* are constants that depend on the physical characteristics of ice. The parameter x_0 describes the exposure for a given design curve.

Although there was variation in the nominal contact area for each lifeboat-ice interaction event, *a* constant instrumented area was considered for each of the stem load panel and bow shoulder load panel, which were estimated using the width of the panels and the

average ice thicknesses. The estimated nominal panel area was 0.1496 m^2 for the stem load panel and 0.3420 m^2 for the bow shoulder panel at the given average ice thickness of 0.38 m in 2013 ice trials. During 2014 ice trials, the measured average ice thickness was 0.51 m, which gives panel areas of 0.2008 m^2 and 0.4590 m^2 for the stem load panel and bow shoulder panel, respectively.

This analysis was completed for the loads that occurred at the TEMPSC stem and bow shoulder independently, resulting in two unique plots of local pressure. For this analysis, emphasis is on the peak loads measured in a given ice concentration level.

4.3.2   Analysis of Stem Loads

As this analysis is driven by an interest in design loads, the analyses are performed using the top 20% loads measured at each ice concentration category, based on the event-maximum method of local pressure estimation (Jordaan et al., 1993; Taylor et al., 2010). The local pressure curves representing the top 20% stem loads for 2013 tests are provided in Figure 4.17. As area is constant and the ice thickness is consistent for all events, α is expected to be approximately constant for the extreme pressure curve. The x_0 parameter reflects exposure, which changes for different ice concentration.
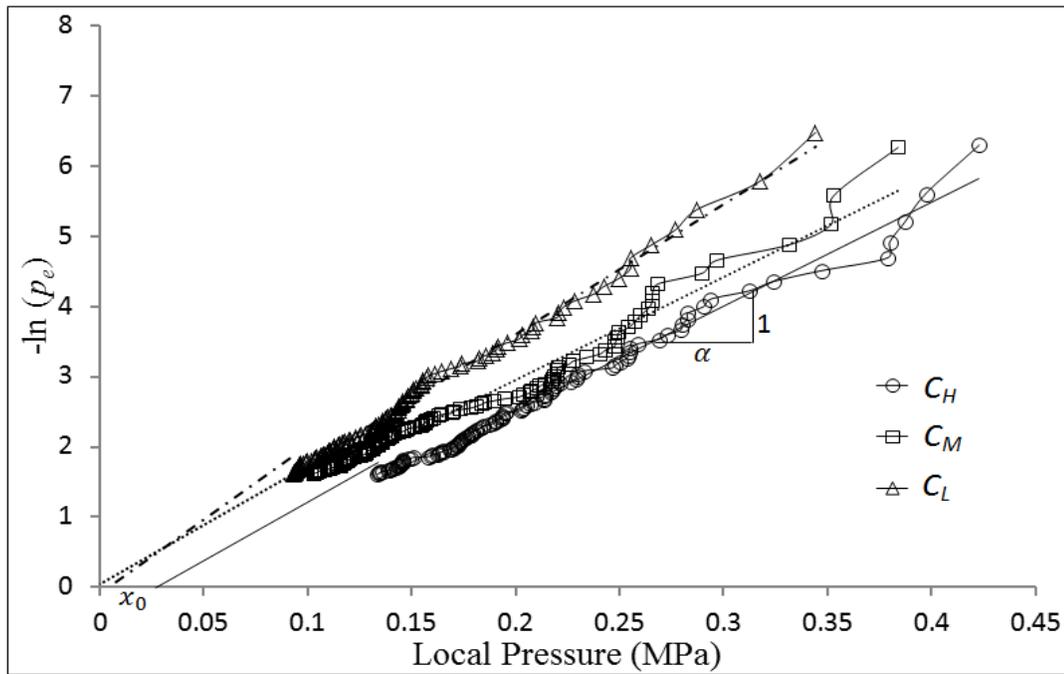
Figure 4.17: Local pressure curve for impact events on the stem (2013)

The local pressure curves representing the extreme values measured on the stem for 2014 tests are provided in Figure 4.18. There does not appear to be significant difference between the high, medium, and low ice concentration categories in the lower local ice pressure range. On the mid-high end of the local pressure range, the low, medium, and high categories become more distinct and have uniquely defined trends.
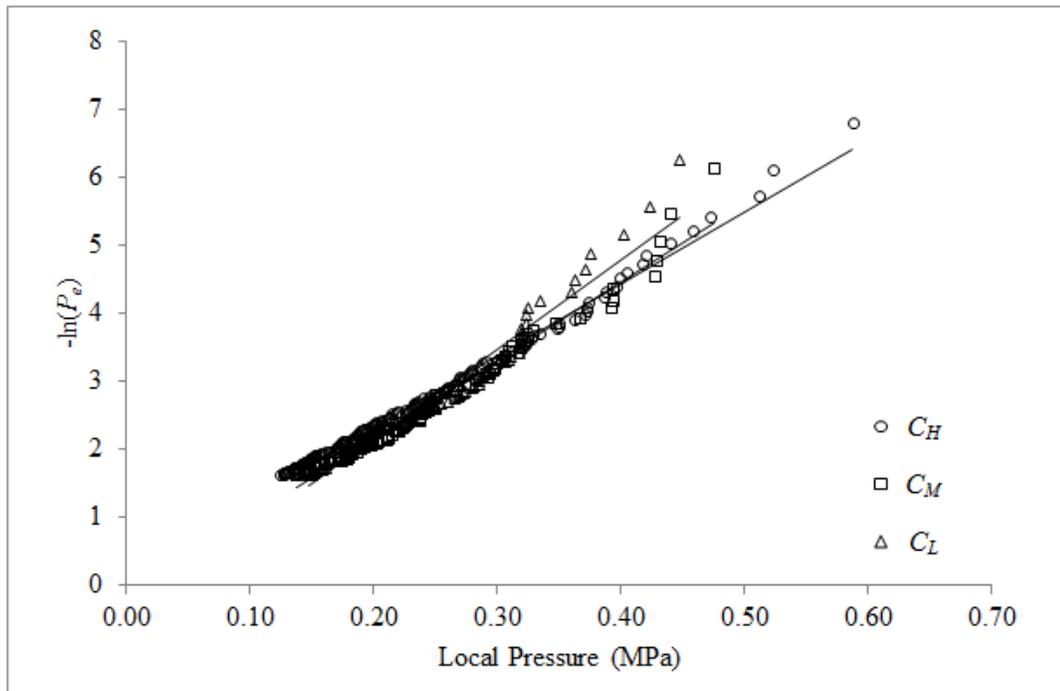
Figure 4.18: Local pressure curve for impact events on the stem (2014)

The α and x_0 values representative of the 2013 and 2014 data, for each ice concentration category, are summarized in Table 4.3.

Table 4.3: Parameters estimated from local pressure curve (2013 and 2014 stem loads)

Ice concentration	Stem loads 2013		Stem loads 2014	
	α	x_0	α	x_0
C_H	0.068 MPa	0.029 MPa	0.095 MPa	0.020 MPa
C_M	0.068 MPa	-0.002 MPa	0.087 MPa	-0.014 MPa
C_L	0.054 MPa	0.006 MPa	0.076 MPa	-0.008 MPa

The 2013 data for each ice category was compiled to develop a general local stem pressure curve representative of ice loads from all ice concentrations. This result was compared to a similar plot which was created for data resulting from the field trials

conducted in 2014. During 2013 field trials, the mass of a single ice piece was on the order of one times the mass of the fully loaded TEMPSC and thus smaller than the average ice piece mass in 2014 (by a ratio of 1:1.25). The general local stem pressure curves resulting from both 2013 data and 2014 data are provided in Figure 4.19. The local pressure curve for the stem based on 2013 data is distinctly different from that based on 2014 data. Both curves have strong trends with few outliers.
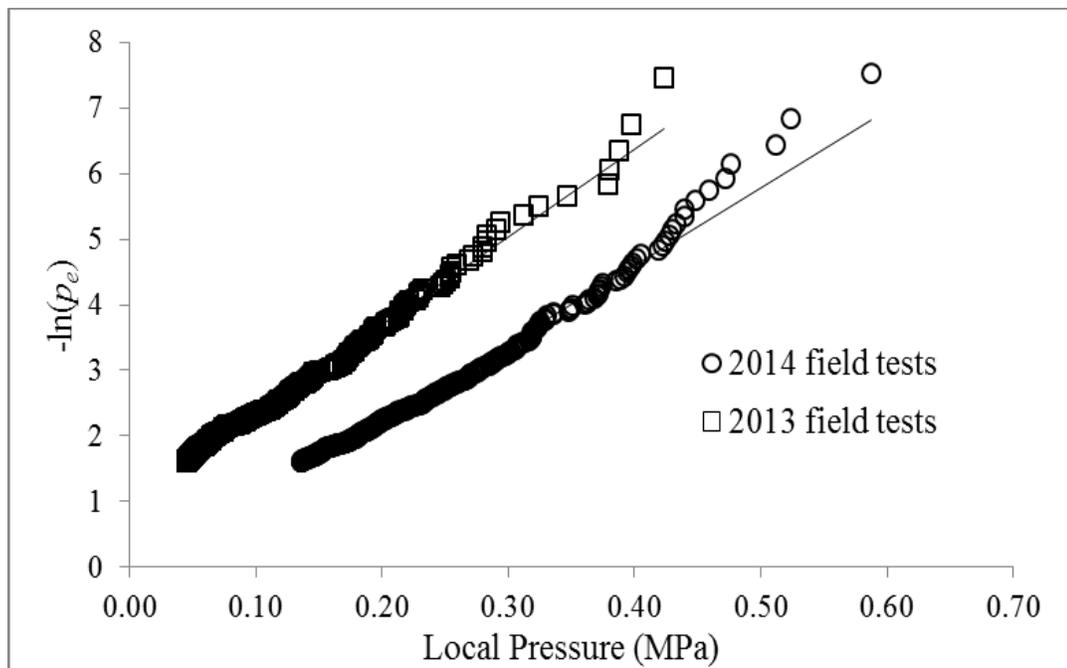
Figure 4.19: Comparison of local pressure for impact events on the stem measured in 2013 and 2014 field tests

4.3.3   Analysis of Bow Shoulder Loads

The extreme values within the tail portions of each bow shoulder histogram were used to devise a local pressure curve representative of the bow shoulder. The pressure curves for bow shoulder loads are plotted in Figure 4.20 and Figure 4.21 for 2013 and 2014 field

tests, respectively. The local pressure values for the bow shoulder are much smaller than the pressure values for the stem.
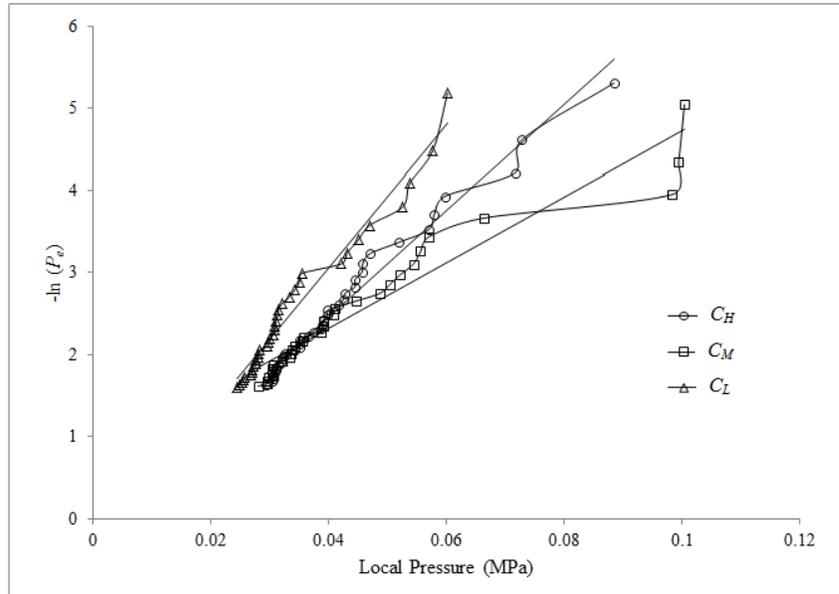
Figure 4.20: Local pressure curve for impact events on the bow shoulder (2013)
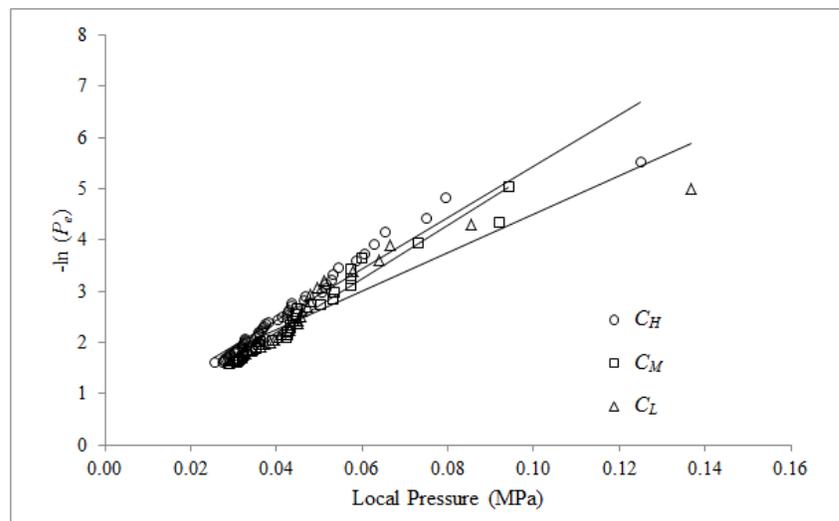
Figure 4.21: Local pressure curve for impact events on the bow shoulder (2014)

Consistent with the analysis process for the stem loads, the local pressure values for each ice concentration category were compiled to allow for development of a general local pressure curve. This general curve is representative of extreme 20% ice loads measured in all ice concentrations during 2014 field trials. This result was compared with a similar local pressure curve for the bow shoulder that was devised based on 2013 data. Both local pressure curves are provided in Figure 4.22.
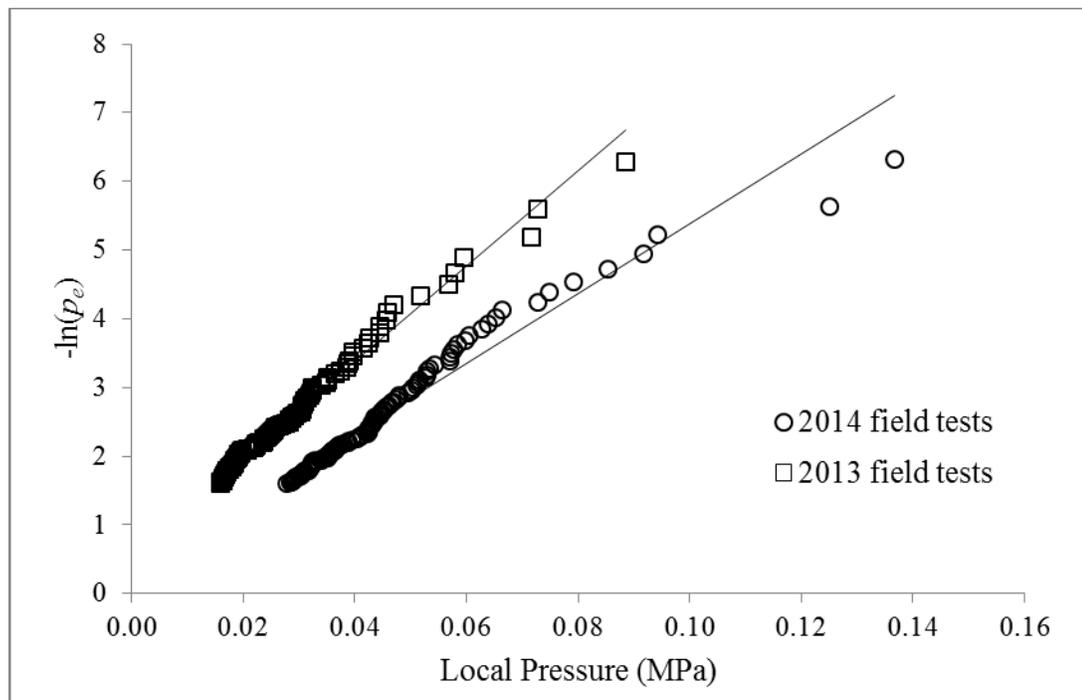
Figure 4.22: Comparison of local pressure for impact events on the bow shoulder measured in 2013 and 2014 field tests

Similar to the 2013/2014 comparison of local stem pressure curves in Figure 4.19, the local bow-shoulder curve for 2013 was distinctly different from that resulting from 2014 data. The α and x_0 values representative of the bow shoulder for the 2013 and 2014 data

are provided in Table 4.4. These values define the local bow shoulder pressure curves for each ice concentration category. The alpha value does not consistently increase or decrease with increasing ice concentration for the bow shoulder data. This is different from the alpha values from the stem load analysis.

Table 4.4: Parameters estimated from local pressure curves (2013 and 2014 bow shoulder loads)

Ice concentration	Bow shoulder loads 2013		Bow shoulder loads 2014	
	α	x_0	α	x_0
C_H	0.015 MPa	0.002 MPa	0.020 MPa	0.009 MPa
C_M	0.025 MPa	-0.018 MPa	0.019 MPa	0.002 MPa
C_L	0.011 MPa	0.005 MPa	0.027 MPa	0.020 MPa

4.3.4 Exposure

The exposure of the vessel is an important consideration in assessing the extreme load. One important aspect of exposure is the number impact events that the vessel will encounter during a given time period. The number of impacts can be depended on a variety factors such as the ice conditions (e.g. ice concentration, floe size), the required sail-away distance, the threshold chosen for impact events. The effects of these factors are discussed below.

4.3.4.1 Ice Conditions

An example is presented here to illustrate the effect of ice concentration and ice floe mass on the number of impacts. In defining example scenarios, the total sail-away distance was calculated by adding the sail-away distance values measured from each test in a given ice concentration category. The total number of interaction events for each ice concentration

category was found by taking the sum of the total number of interaction events for each test in that given category. The average number of interaction events v' per kilometer, was then estimated by taking the total number of events and dividing by the total sail-away distance. This was calculated for low, medium, and high ice concentrations and the corresponding values are summarized in Table 4.5, for both 2013 and 2014 data. The actual distance (path length) transited may be larger than the sail-away distance, particularly for high ice concentrations where coxswains have to find their way through small leads in the ice. The effect of such deviations is reflected in the larger number of impacts that will occur in the process of moving from the platform to the rescue vessel.

Table 4.5: Number of interaction events on the stem for different ice concentrations (2013 and 2014 tests)

Number of events	2013 tests			2014 tests		
	C_L (4-5)	C_M (6-7)	C_H (8-9)	C_L (5)	C_M (6-7)	C_H (8-9)
v' (per km)	250	450	650	750	1150	1550
v (0.5 km)	125	225	325	375	575	775
v (1.0 km)	250	450	650	750	1150	1550
v (5.0 km)	1250	2250	3250	3750	5750	7750

A comparison of estimated number of impacts per kilometer of sail-away distance at the stem for two data sets, 2013 and 2014, is shown in Figure 4.23. The level of exposure (number of impacts) increased with rising ice concentration, which indicates that the possibility of encountering ice impacts rises as the lifeboat passes through a denser pack ice region. In addition, the comparison of 2013 to 2014 data indicates that for the thicker ice conditions, a higher number of impact events with load levels exceeding the threshold occurred at each ice concentration level. The movement of the lifeboat through ice during

2014 trials was limited by the ice floes having a larger average mass than those in the 2013 trials, which resulted in a larger number of impacts and lower sail-away distances.
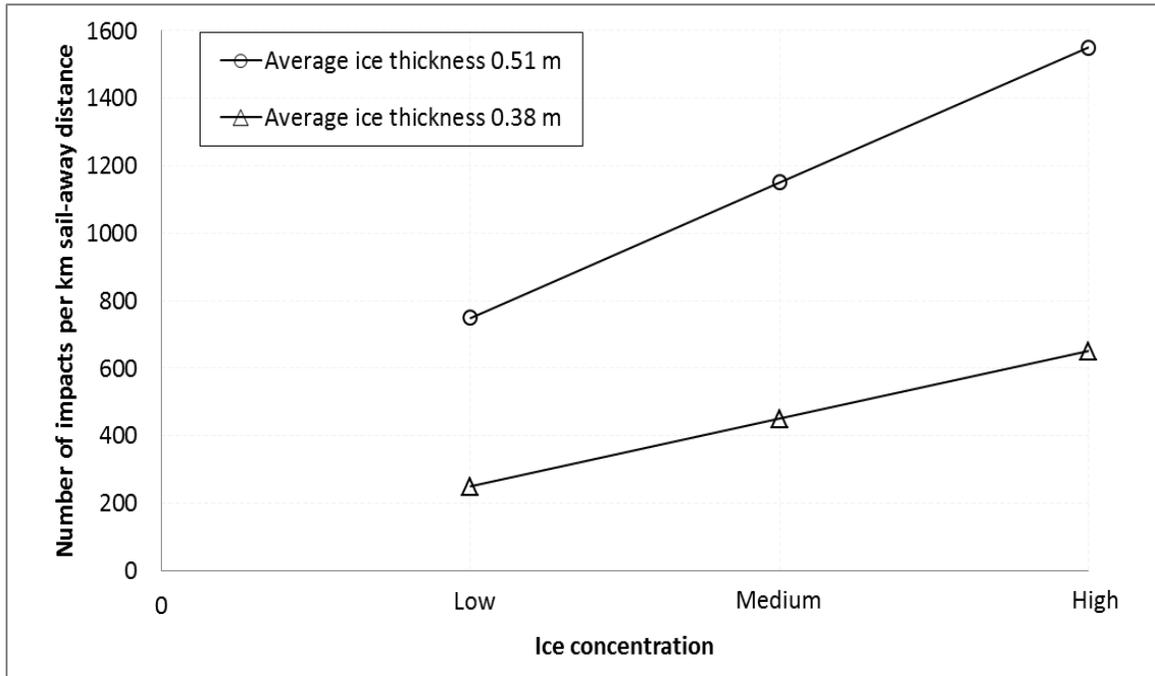
Figure 4.23: Comparison of expected number of ice impacts per km sail-away distance at stem area in two different ice thicknesses

Navigation of small vessels through pack ice will be sensitive to local variations of ice concentration. In applying this method, one must consider the local ice concentration as the individual floe sizes (mass) will have a big effect on resulting ice loads. Typically, ice concentration reflects an average areal distribution of ice in a region. As depicted in Figure 4.24, different spatial configurations of ice will present very different operating environments. This also affects the number of impacts per km sail-away distance, which in turn influences design loads estimates.

Ice   Water
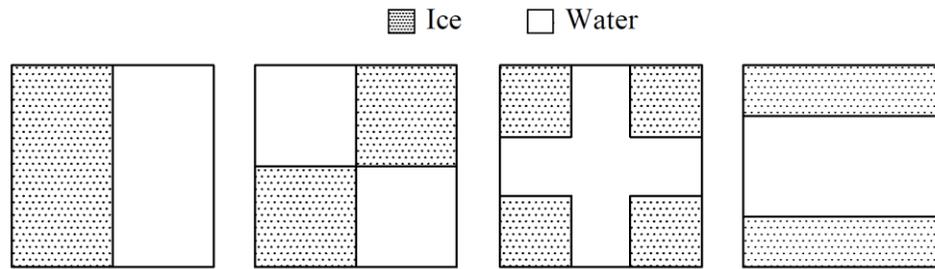
Figure 4.24: Idealizations of different ice floe configurations of 5/10ths ice concentration

4.3.4.2 Sail-away Distance

It is important to consider how the exposure is defined in terms of sail-away distance and the ice concentration. To simplify the discussion, if we assume that each impact event corresponds to essentially a single floe-ship interaction we can illustrate, as shown in Figure 4.25, the relationship for (a) constant exposure, different sail-away distance and (b) different exposure, constant sail-away distance in different ice concentration levels. In the first case illustrated in Figure 4.25 (a), as the ice concentration increases, the vessel only needs to transit a shorter sail-away distance to be exposed to the same number of impacts. In the second case in Figure 4.25 (b), if the vessel is transiting a fixed sail-away distance, we expect exposure to increase as ice concentration increases. In applying the techniques presented in the preceding section, it is essential that a consistent basis is used in correctly defining exposure which typically will correspond to the case of fixed sail-away distance, not a fixed number of impacts.

(a) Constant exposure (Constant number of impacts, different sail-away distance)

C_H

C_M

C_L
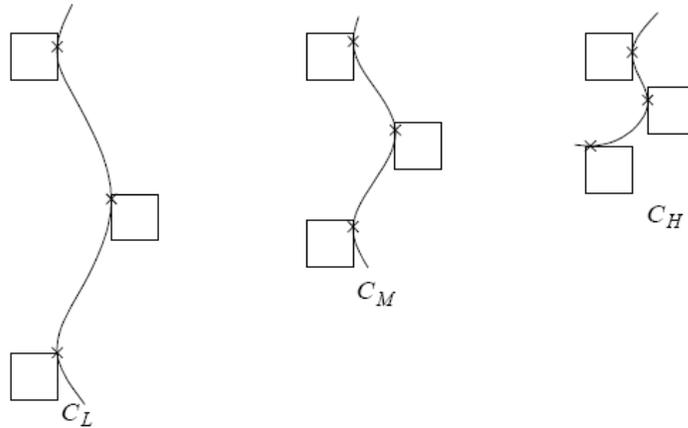
(b) Different exposure (Constant sail-away distance, different number of impacts)

C_L C_M C_H
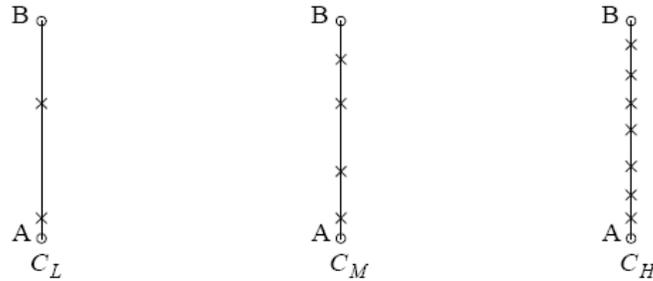
Figure 4.25: Effect of number of impacts and sail-away distance on exposure

4.3.4.3 Threshold Effects

For analyzing the data, a minimum ice load threshold of 4 kN was set for both 2013 and 2014 tests. In thicker ice (2014 tests), there were more events above the threshold as depicted in the Table 4.5. For thicker ice interactions, more impact events will result in loads that exceed the 4 kN threshold which results in larger numbers of events registering on the load panels (i.e. stem and bow shoulder). This threshold effect is illustrated in Figure 4.26, in which the loads measured above the threshold are plotted against test time for two individual tests during 2013 and 2014 field trials. Both tests were performed in 5/10ths ice concentration and travelled similar sail-away distance. In 2014 tests, the lifeboat had longer path length, time on course (due to the heavier ice floes) and

experienced higher number of impacts than 2013 test, of which a significant number were just above the threshold load value.
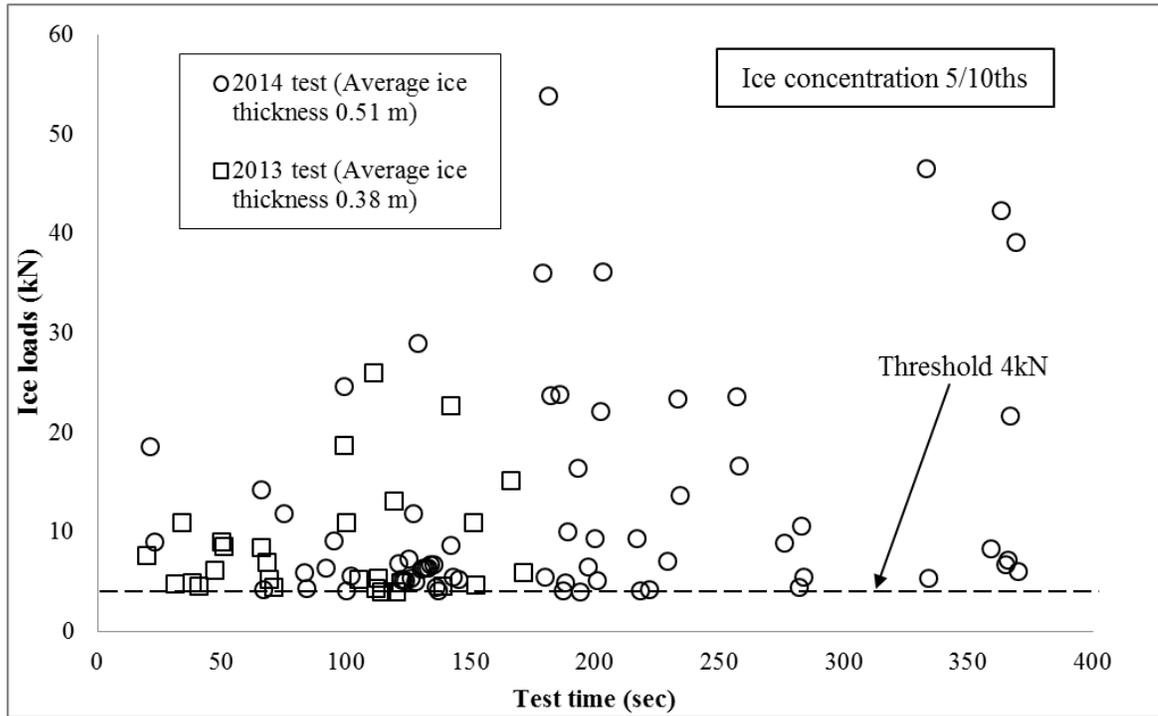
Figure 4.26: Threshold effect on the number of impacts in 2013 and 2014 test at 5/10ths ice concentration

If a load (force) threshold is used in the analysis, as the ice thickness increases, the number of events exceeding threshold will also increase. For example, the vessel may nominally come into contact (impact) 1000 ice features, but for the case of thin ice only 250 of those may register a load above 4kN, whereas for thicker ice 650 events may register a load above the threshold. To improve consistency in event definition, which in turn is reflected in the total estimated number of impacts during a trial, use of a threshold

pressure instead of force is recommended in future analyses, since the threshold value will then be normalized by the ice thicknesses.

4.3.5 Illustrative Example

To illustrate how the results may be used to estimate local design pressures for the stem, the event-maximum method is used to estimate the extreme pressure z_e using the following equation:

$$z_e = x_0 + \alpha\{-ln[-ln\,F_Z(z_e)] + ln\,v + ln\,r\} \tag{4.2}$$

where α and x_0 are constants, $F_Z(z_e)$ is the exceedance probability, v is the expected number of events and r is the expected proportion of impact loads on the given region. In this method, α is generally taken as an area dependent relationship that is determined from ship-ice impact data given by the expression:

$$\alpha = Ca^D \tag{4.3}$$

where the coefficients C and D are empirical constants determined from ship-ice impact data (Taylor et al., 2010). For the present study, it is not possible to develop such an area-dependent relationship, since loads have only been collected for a single panel area at the stem/bow shoulder.

Using values α and x_0 from Table 4.3, the values for the expected number of events ν given in Table 4.5, and assuming the expected proportion of ice impacts on the stem, r, is 0.5 (e.g. 50% of the impacts occur on the stem panel, while all others occur on the sides or elsewhere on vessel), and assuming $F_Z(z_e)$ corresponds to a probability of exceedance of 10^{-2}, we get estimates of the extreme pressures for the stem, summarized in Table 4.6.

Table 4.6: Local design pressures at stem for example scenario

Transit distance (km)	Stem local design pressures (MPa) for different ice concentrations and transit distances					
	2013 tests			2014 tests		
	C_L (4-5)	C_M (6-7)	C_H (8-9)	C_L (5)	C_M (6-7)	C_H (8-9)
0.5 km	0.48	0.63	0.69	0.74	0.88	1.02
1.0 km	0.52	0.68	0.74	0.79	0.94	1.09
5.0 km	0.60	0.79	0.84	0.91	1.08	1.24

The extreme design pressures at the stem were calculated based on the 2013 and 2014 data set separately. The design pressure values based on 2013 data and 2014 data are each illustrated in Figure 4.27 for the 1.0 km transit distance case. Design pressure values are provided for each category of ice concentrations: low, medium, and high.
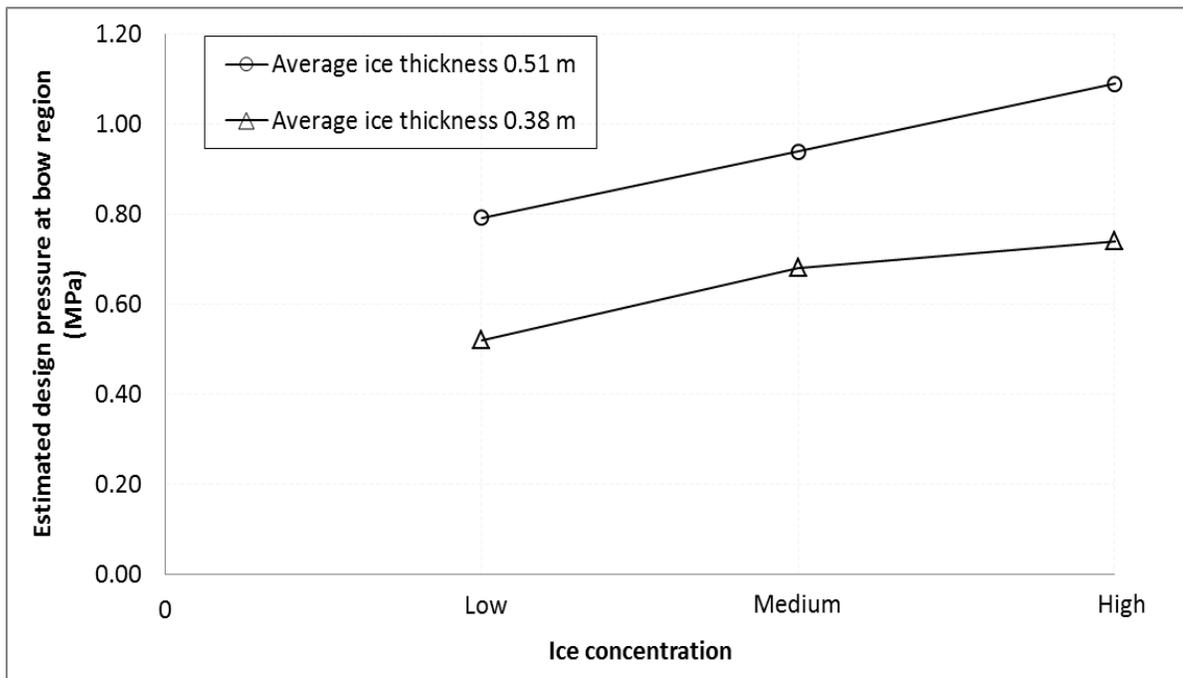
Figure 4.27: Comparison of estimated design pressure at stem for two different ice thicknesses

The design pressure guidance based on 2014 field results is distinctly higher than that from 2013 testing results. This indicates that the design pressure should be higher for thicker (heavier floes) ice conditions. These design pressure values can be used to guide the design of ice capable evacuation craft and other GRP vessels that operate occasionally in ice. It should be cautioned that more severe conditions, including thicker ice floes and floes with larger mass would likely require a higher design pressure. This result reflects the importance of remembering that when using empirical approaches as presented here, the parent distributions associated with a given set of measurements are reflective of that particular data set, which in turn is associated with a given combination of structural configuration and ice conditions, and not an underpinning physical law that can be

universally applied. As a consequence one must exercise a high degree of caution in extending those data to structure-ice combinations other than those embodied in the data.

4.3.6   Discussion of Results

The stem loads result in local pressure curves that are unique for high, medium, and low ice concentrations. These local pressure curves each represent different pressure levels and are defined with unique α values that increase with increasing ice concentration (e.g. exposure). In contrast, the bow shoulder loads result in intermingled local pressure curves for the low, medium, and high ice concentrations. The α values do not increase with increasing ice concentration. Therefore, a specific local pressure curve relevant to a certain range of ice concentrations may be used to guide the design pressure for the TEMPSC stem whereas a generic local pressure curve may be more relevant for the bow shoulder.

The peak bow pressure measured for all events during 2013 and 2014 field programs was about 0.42 MPa and 0.59 MPa, respectively. From Table 4.6 it is observed that the local design pressure for low ice concentrations and short transit distances corresponding to an exceedance probability of 10^{-2} is 0.48 MPa and 0.74 MPa for 2013 and 2014 tests, respectively, which is greater than the measured peak bow pressure. This result suggests that the proposed method provides a conservative estimate of design pressure for the conditions considered in this study.

A comparison of the results of the probabilistic evaluation of 2014 data with 2013 data indicated a number of distinct differences. The level of exposure, or number of ice impacts above a given threshold at a given ice concentration level, was larger for an ice field with higher average ice piece mass. In addition, the magnitudes of peak ice loads measured in the higher ice piece mass cases (2014) were larger than those measured in an ice field with smaller average ice piece mass (2013). These two factors lead to higher design pressure values for the ice conditions with larger ice piece mass. For the high level ice concentration, the design pressures based on 2013 and 2014 data differ by approximately 0.35 MPa. In general, the estimated design pressure for the 2014 tests is on average 1.46 times greater than the 2013 test for the ice mass ratio of 1.34.

For design pressure estimation, focus is on the tail of the ice load distribution. Here the analysis was performed considering the top 20% loads of each histogram. A sensitivity analysis was also performed to examine the influence of extreme load sample size used to estimate the design curve parameters (α and x_0) for design pressure estimation, which is presented in Table 4.7 for 2013 stem loads. It is found that there was no significant change of design pressures for different percentage of extreme loads. However, too small (e.g. less than top 10%) or too large (e.g. more than top 30%) sample size may result misleading design parameter estimates.

Table 4.7: Stem local design pressures (MPa) considering different percentage of extreme stem loads of 2013 tests

Transit distance (km)	Stem local design pressures (MPa) based on the stem loads of 2013 tests								
	C_L (4-5)			C_M (6-7)			C_H (8-9)		
	10%	20%	30%	10%	20%	30%	10%	20%	30%
0.5 km	0.48	0.48	0.48	0.60	0.63	0.64	0.68	0.69	0.69
1.0 km	0.51	0.52	0.51	0.64	0.68	0.69	0.73	0.74	0.74
5.0 km	0.60	0.60	0.60	0.74	0.79	0.80	0.84	0.84	0.85

The vessel characteristics, such as structural aspects of the fiberglass hull (e.g. panel stiffness), panel area, as well as possible refreezing of managed ice fields on design loads, are also areas identified for investigating their influence on the ice loads. Stiffness of the vessel is a critical consideration on design ice loads as stiffening the structure may significantly increase the resulting ice loads. The interaction time and the deflection of the hull are relatively higher for composite structure vessels than stiff steel structures. For instance, if we consider that a given ice mass dissipates all of its kinetic energy doing work in deflecting a local panel, as illustrated in Figure 4.28, we see that a stiff structure will develop higher forces over a shorter distance (and period of time) to absorb the same amount of energy than would be the case for a compliant structure. This is an important consideration for future work, particularly in considering how these data relate to stiffer or larger vessels. Further research is recommended to investigate and quantify these effects in greater detail.
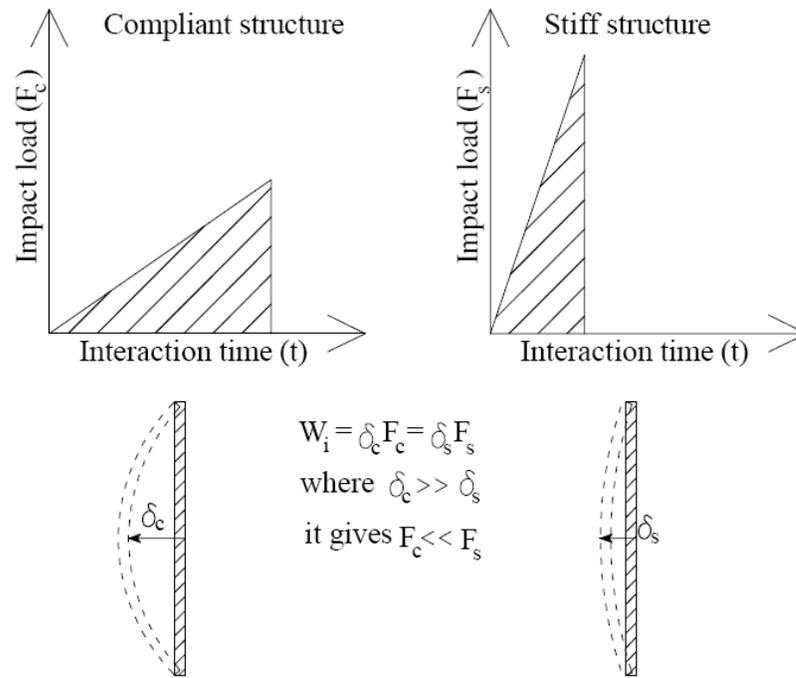
Figure 4.28: Impact load profile and deflection of compliant and stiff structure

4.4 Concluding Remarks

The design pressure analysis presented in this chapter provides insight as to how the design pressure could change for different ice concentrations and sizes and suggests a methodology for calculating these values for different environmental and operating conditions that the craft will be exposed to over its design life.

5 Effects of Operational Parameters on Performance

5.1 Scope

This chapter is focused on the parameters that affect operational performance, with the aim of promoting safety through insights how to improve training so that coxswains can be taught best practices for operating in ice. Operational parameters considered include coxswain experience, transit speed, and propeller speed. Coxswains with different levels of experience and backgrounds operating in ice may employ different navigational strategies (e.g. aggressively impacting the ice versus cautiously weaving through gaps between floes), resulting in significant differences in the loads on and motions of the vessel (Billard et al., 2014). More aggressive strategies can be expected to increase the exposure of the vessel to higher loads and to more severe motion. Further, these factors are also considered in terms of their effect on lifeboat transit distance as this is another area of weakness in terms of lifeboat operational capabilities in Arctic conditions. Essentially, the variation of these factors (coxswain experience, transit speed, and propeller speed) may mitigate or reduce the magnitude of ice loads that a lifeboat experiences when it maneuvers through an ice field. The same factors may also have the potential to decrease the capability of the lifeboat to transit through an ice field.

5.2 Approach

The coxswains who participated in the trials had different levels of experience operating small crafts and operating in ice covered waters. Included in the study were individuals with experience as operators of large vessels (icebreakers and fishing vessels), Fast

Response Craft (FRC) crew members, and offshore oil and gas lifeboat coxswains. Candidates for the trials were interviewed and asked to provide information on the amount of experience operating small craft (less than 15m or less than 25 gross tonnes), and the amount of experience operating vessels in ice covered waters. The participants ranged from icebreaking captains with limited time spent on small vessels, to small craft operators who were very familiar with the handling of small vessels, but who had limited experience maneuvering through ice. Table 5.1 summarizes the category of coxswains based on their experience.

Table 5.1: Coxswain experience categories

Legend item	Experience
EL	Lifeboat operators with experience in ice.
SC	Small craft operators – limited experience operating in ice
LV	Large vessel operators – experience operating icebreaking vessels in ice, limited small craft experience

The participants in the trials were asked to use an approach that they felt the most appropriate for navigating through the pack ice. As a result, different tactics were used. Each participant did 5 to 7 trials in ice fields of concentrations ranging from 5/10ths to 8/10ths. Following the trials, the participants were interviewed to provide details on the technique they used and their strategy during the tests. A second set of trials was done with operators who were considered to have significant experience operating lifeboats in ice. This included subjects who had participated in lifeboat testing trials in both fresh water and salt water ice fields (Simões Ré et al. 2008 & 2011, Kennedy et al. 2010, Simões Ré et al. 2012). The maneuvering techniques and results of the first time drivers

and the operators with significant experience were compared to determine the impact of experience and background.

Seven benchmarks were selected for analyzing the performance of lifeboat: propeller speed, stem load, bow shoulder load, roll, pitch, path length and sail-away ratio, and mean speed. These benchmarks were used to study the influence of different driving styles and techniques on the load magnitude experienced by the lifeboat, crew comfort, and ability of the coxswain to maneuver through ice. Only the average and maximum of these benchmarks are considered to show the general trend.

5.3   Results

Results are presented on radar plots, as shown in Figure 5.1 to Figure 5.8, which are plotted for several ice concentrations in the trials. The driving style for the operator is indicated by the average propeller speed, which is presented on axis 1 of the radar plot. A high mean propeller speed suggests the operator maintained a high throttle and used an aggressive approach. The other axes show the results of the loads and motions. The impact loads on the bow shoulder and stem of the vessel are shown on axis 2 and axis 3, while axis 4 and axis 5 show the roll and pitch motions of the lifeboat. Results are presented as averages and maximums for different ice concentrations. For presentation purposes, maximums are plotted with a different scale than the averages.

Axis 6 and axis 7 indicate the ability of the operator to maneuver through the ice effectively and average speed of transit. One of the performance measures is how straight a path the coxswain takes during transit. This distance differed depending on whether the operator was asked to drive the length of the test site (86 m) or the width of the test site (38 m) or any oblique angle. A high path length distance (PL) to sail-away distance (SA) ratio indicates the lifeboat had to perform more turns to maneuver through the ice field, as opposed to a PL/SA ratio of 1.0, which means the vessel maintained a constant heading and was not required to veer off course to reach the safe zone. This ratio was used to make comparisons between trials of different PL and SA. The PL/SA ratio is illustrated on axis 6 of the radar plot. The mean speed of the operator is plotted on axis 7 and indicates the pace at which the operator was able to maneuver through the ice field.

The results show that different driving techniques influence the ice loads and lifeboat's motion. If we consider coxswain EL1 in 5/10ths ice cover (Figure 5.1 and Figure 5.2), the driving behavior indicated low propeller speed, which resulted in relatively low heave and roll motions and impact loads. The driver also had a lower mean average speed than other cases. Compared to this coxswain, some drivers were more aggressive and others were more conservative. Driver LV2 had a higher average throttle and experienced higher stem loads and roll motions, while achieving a higher mean speed. Driver LV3 had a lower average throttle and much lower impact forces and motions. This driver had a higher PL/SA ratio, indicating the driver maneuvered through the ice with multiple turns, even in low ice concentrations. As a result, this coxswain achieved a much lower mean speed than other coxswains.
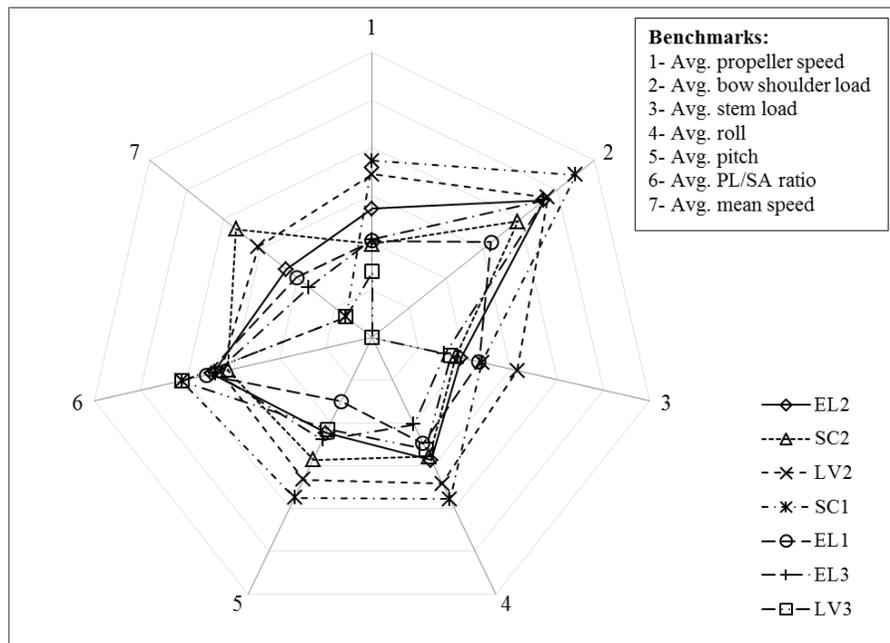
Figure 5.1: Average of benchmarks for different coxswains at 5/10ths ice concentration
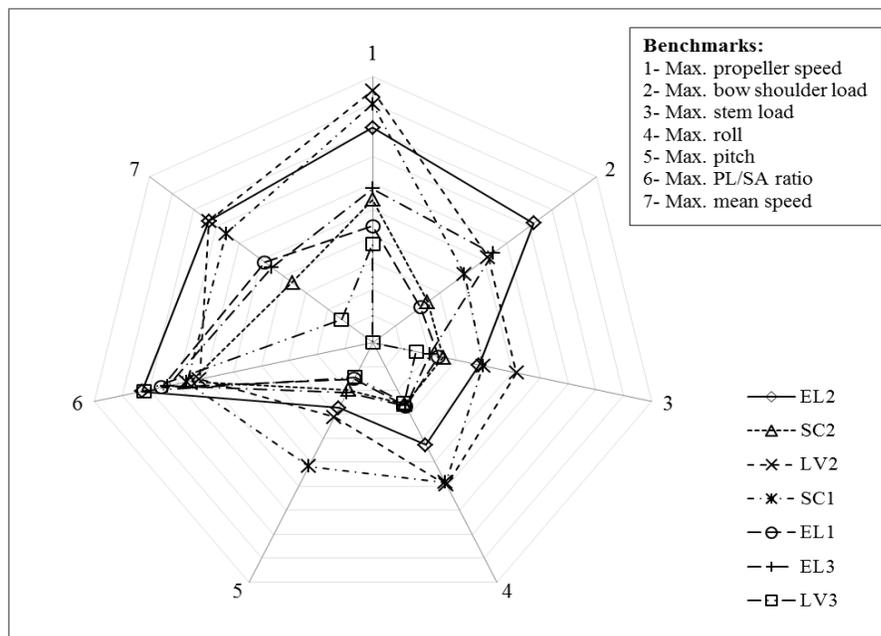
Figure 5.2: Maximum of benchmarks for different coxswains at 5/10ths ice concentration

Similar results are found in higher ice concentrations, which required a more tactical approach. Previous studies (Simões Ré and Veitch 2003, Simões Ré et al. 2008 & 2011, Kennedy et al. 2010, Simões Ré et al. 2012) indicated that lifeboat coxswains can maneuver through ice up to 7/10ths ice cover, although maneuvering techniques may need to be adjusted in higher concentrations. Figure 5.3 to Figure 5.6 illustrate that different tactics were used in medium ice concentrations, with overall propeller speed being reduced, which resulted in lower mean speeds through the ice. If we consider the individual behaviors of the drivers again, coxswain EL1 used a more aggressive throttle than other operators. In the 6/10ths ice cover, this operator achieved the highest mean speed, and the driving style also resulted in higher impact forces, and roll and pitch motions. Driver LV3 continued to use a conservative approach in 6/10ths and 7/10ths ice cover and minimized the forces on the lifeboat while also achieving the lowest mean speeds. Each of the operators achieved a similar PL/SA ratio in 6/10ths ice cover regardless of the technique that was used.
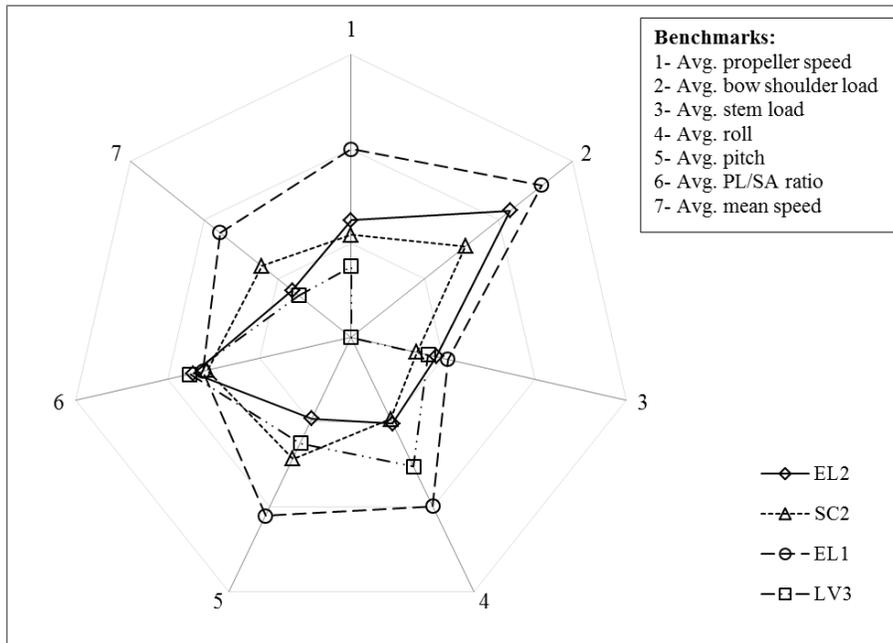
Figure 5.3: Average of benchmarks for different coxswains at 6/10ths ice concentration
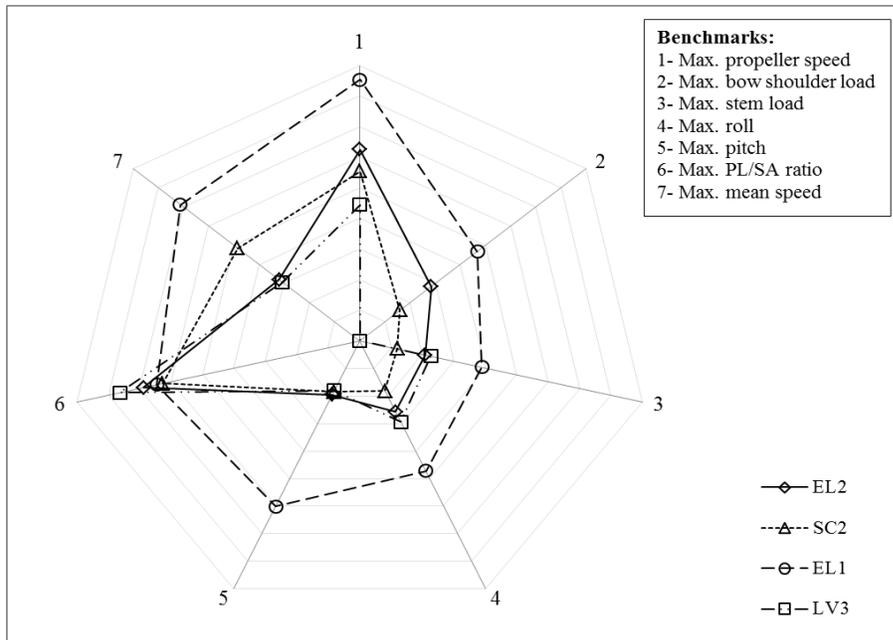
Figure 5.4: Maximum of benchmarks for different coxswains at 6/10ths ice concentration

In 7/10ths ice cover (Figure 5.5 and Figure 5.6), it is apparent that driving style had a significant impact on the results. Operator EL1 used an aggressive throttle, and as a result had higher bow and side impact forces, and pitch and roll motions. Unlike in lower ice concentrations, this style did not result in the highest mean speed. EL2, another experienced lifeboat operator, used a less aggressive approach and made several turns in the ice, as indicated by the high PL/SA ratio. This operator achieved a similar mean speed through the ice, and higher maximum speed, and was able to maneuver through the ice field with reduced impact forces and vessel motions. The lowest impact forces and vessel motions were achieved by operators who kept their maximum propeller speed low, and in most cases the operators achieved a higher mean speed through the ice field. The highest mean speeds were achieved by large vessel operators (LV1 and LV2), who appeared to use a plowing approach to push through the ice.
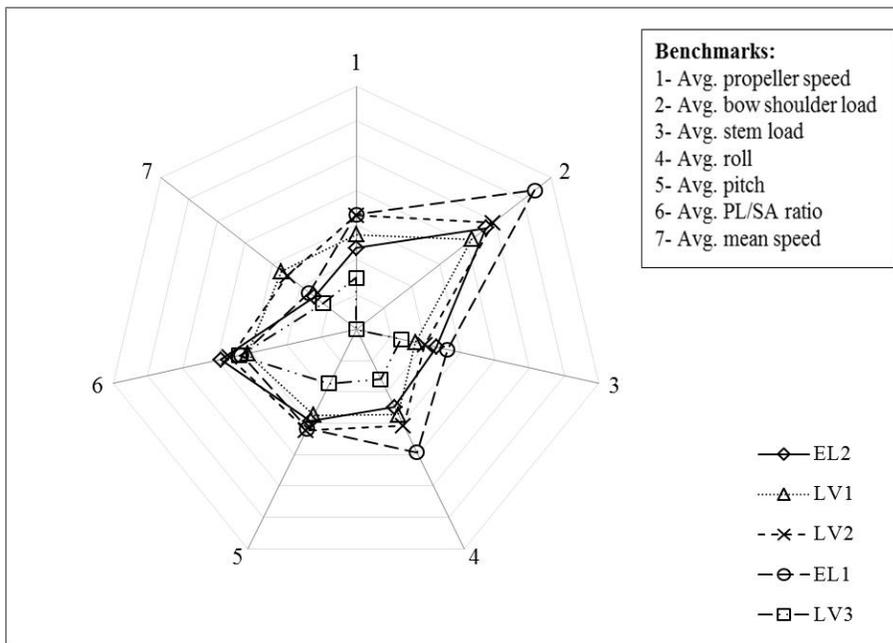
Figure 5.5: Average of benchmarks for different coxswains at 7/10ths ice concentration
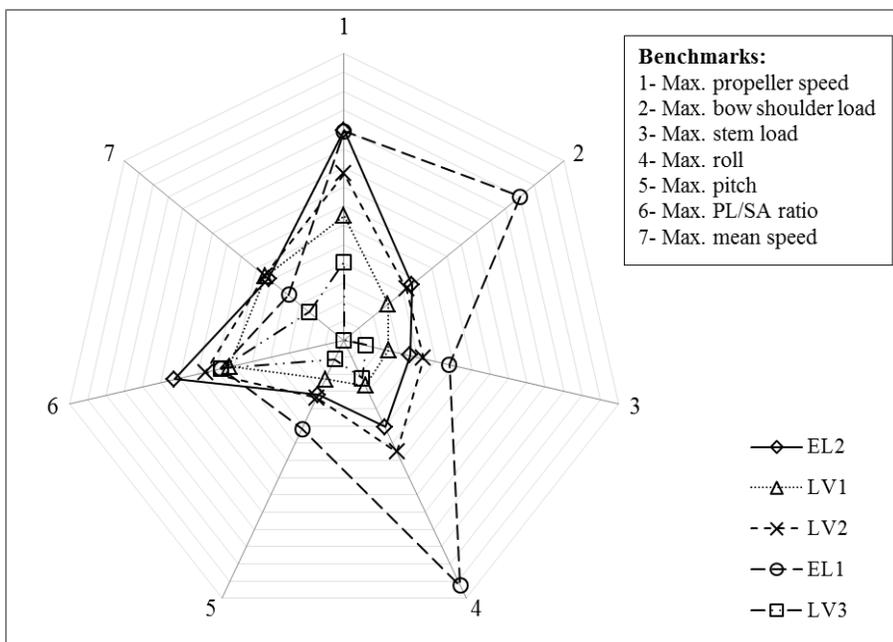
Figure 5.6: Maximum of benchmarks for different coxswains at 7/10ths ice concentration

For 8/10ths ice cover (Figure 5.7 and Figure 5.8), the results show that the environment had an impact on performance, as the mean speed through the ice was reduced for most operators. A variety of approaches were used to maneuver through the high ice concentration. One of the more experienced operators (EL2) used many turns to push the ice and keep the vessel moving, as indicated by the high PL/SA ratio. Lower overall speeds were achieved in this higher ice concentration.
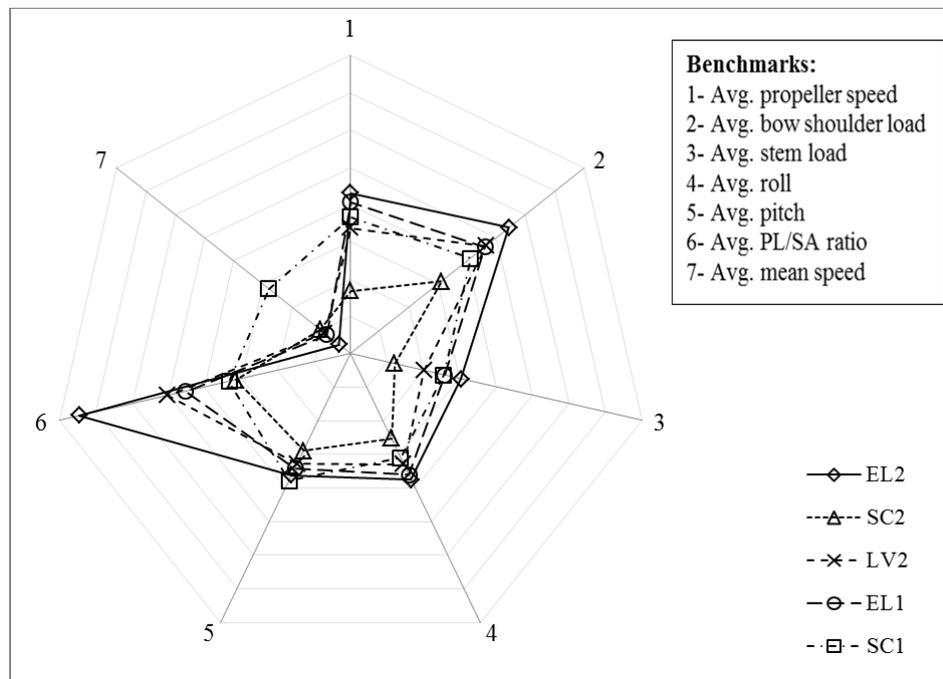

Figure 5.7: Average of benchmarks for different coxswains at 8/10ths ice concentration
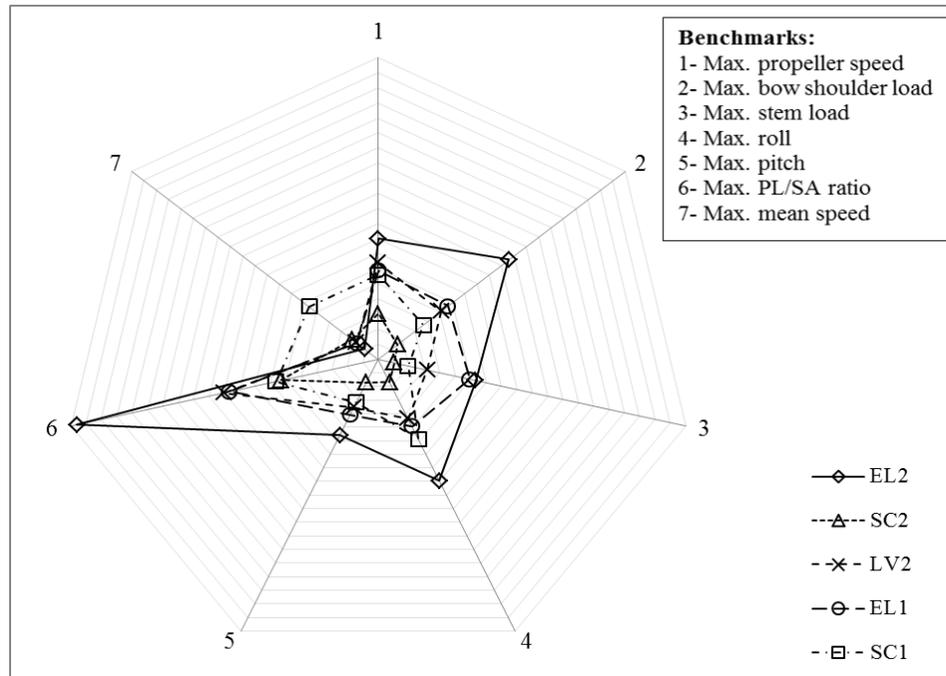
Figure 5.8: Maximum of benchmarks for different coxswains at 8/10ths ice concentration

It was evident that the coxswains reduced their throttle (propeller speed) in higher ice concentrations. The level of difficulty of maneuvering through the pack ice increased as the concentration increased, which is an expected outcome. Post-trial interviews with the participants indicated they were more concerned with the impact on the vessel and their crew in the higher ice concentrations, and they changed their approach to maintain the integrity of their craft and comfort of the crew. As an exception, in tests in 7/10ths ice cover, one coxswain who averaged a high shaft speed had resultant impact loads greater than 30 kN and roll motions as high as 40 degrees. Compared to this operator, most of participants achieved a higher mean speed, and a similar PL/SA. This indicates that this aggressive approach did not provide an increase in performance or effectiveness.

Coxswains also noted that a higher throttle was sometimes needed in higher ice concentrations to start pushing ice and to keep the ice moving. More propulsion force was needed when multiple pieces of ice came together and had to be pushed simultaneously, or when ice pieces became wedged in the pack ice. Higher impact forces were experienced in lower ice concentrations. This is due to the higher speeds that are achievable in lower concentrations of ice and the availability of open water. The vessel was able to pick up speed more easily and impacted ice at a higher speed, resulting in a greater impact. The impact loads measured in 2013 trials (less than 70 kN for the bow and side) were lower than the TEMPSC's structural capacity. The local strength of the National Research Council's (NRC) TEMPSC at the bow is approximately 182 kN and the local strength of a conventional TEMPSC in the bow region is approximately 94 kN (Simões Ré et al. 2012). Greater loads can be expected if ice floe sizes are larger, which is evident from the 2014 field trials. The results indicate that different approaches influence the forces on the vessel.

Pitch and roll motions were comparable for the 5/10ths coverage to 7/10ths coverage with most angular motion being less than 15 degrees. In lower ice concentrations, the low roll motion is believed to be due to the characteristic behavior of the boat at higher speeds. In higher ice concentrations, the pitch and roll motions were lower due to the constraint by the ice floes.

Figure 5.9 shows the relationship between ice concentration and average vessel speed, and provides an indication of how maneuvering techniques change in higher ice

concentrations. The plotted symbols are the ice concentration for each test performed, with a 7 meaning the field test was performed in a 7/10ths ice concentration. Each symbol relates to a single test. The ability to move through the ice is influenced by the concentration of ice and the mass of the ice floes. Previous studies (Simões Ré & Veitch 2003, Simões Ré et al. 2008 & 2011, Kennedy et al. 2010, Simões Ré et al. 2012) indicated that lifeboats are able to progress in ice conditions up to 7/10ths ice cover depending on the mass of ice floes. For the present study, the ice floe mass was approximately equal to the mass of lifeboat and maneuvering through concentrations up to 9/10ths was achievable if ice was not constrained.

As illustrated in Figure 5.9, PL/SA ratio decreases exponentially as the mean speed increases in relatively lower ice concentrations. Participants increased the path length to maneuver through higher ice concentrations. In instances where the ice floes were constrained, as in high ice concentrations, the lifeboat was unable to displace the ice. As a result, the coxswains were required to choose an alternative heading to maintain forward progress. Depending on the ice formation, the coxswains changed their target heading to enter a lead in the ice field, or changed their heading to push the ice into areas of open water. The operators were unable to maintain a constant heading and were required to zigzag through the ice field, increasing the path length. In effect, the mean speed through the ice field was reduced.
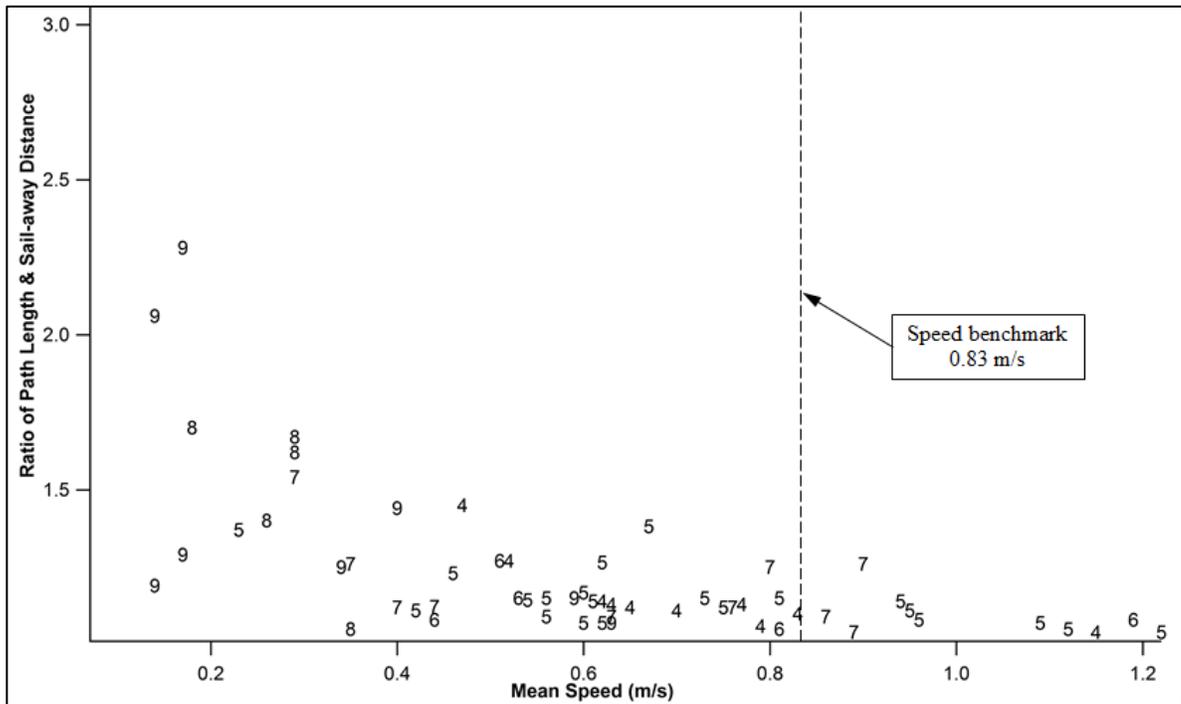
Figure 5.9: Path length and sail-away distance ratio versus mean speed

Previous studies (Simões Ré et al. 2012, Kennedy et al. 2014) defined the mean speed through the ice to be an important measure of whether a lifeboat will be able to proceed to a safe area in an evacuation scenario. If the lifeboat is operating on compressed air (i.e. 10 minutes availability), the goal is to minimize time spent by the survival craft near hazards and to pilot the vessel to a safe zone quickly to avoid depleting breathable air. The time limit of 10 minutes relates to the regulated requirement for a TEMPSC to carry an onboard supply of compressed air (LSA, 2010). The distance limit of 500 m is representative of a typical exclusion zone for an offshore installation. The speed benchmark of 0.83 m/s is defined based on the mean speed required to move 500 m in 10 minutes, which is shown in Figure 5.9. The 2013 test data indicated that the average

transit speed was reduced in higher concentrations. The experimental results suggest that in ice floes of moderate sizes and moderate concentrations (5/10ths to 6/10ths), the average transit speed that can be achieved is around 1.2 m/s or 2.3 knots. If a lifeboat is to maneuver to a zone that is 500 meters from the launch site, it would take approximately 7 minutes to reach the goal. In higher concentrations (7/10ths to 8/10ths), the mean speed was as low as 0.2 m/s and the transit time is significantly increased.

5.4 Discussion

5.4.1 Background Experience and Technique

In terms of technique used in moderate to high ice concentrations, the small craft operators managed the vessel through the ice by trying to impact the ice gently before pushing ice into open water to progress through the pack ice. In post-trial interviews with these operators, they noted that they used an approach to minimize impact forces to preserve the integrity of the lifeboat and to maintain crew comfort. Impacts at speed could damage the lifeboat and introduce roll and pitch motion that could increase crew stress and anxiety. The operators indicated that they found judging their speed and proximity to ice difficult, which sometimes resulted in higher initial impacts with the ice.

Most of the participants with experience operating large craft tried to push ice aggressively and appeared to use the lifeboat as an icebreaker. While this technique allowed them to maneuver through the ice, the operators felt the vessel could handle the high impact forces, and were accustomed to vessels with larger inertias and lower pitch

and roll motions. The large vessel operators were asked to perform a second set of tests using slower maneuvering techniques and they concluded they were able to proceed through the ice by picking ice leads and pushing ice into open water. The operators also concluded that they could still feel the ice being moved even though they used less throttle and impact speeds, which they identified as an important factor in maneuvering through ice fields of high concentrations.

One of large vessel operators, indicated by LV3, used ice management techniques employed by icebreakers, which included using turns and sweeps to push ice away from one side of the vessel. The approach proved to be very successful in reducing the impact force on the vessel as well as minimizing roll and pitch motions. This technique was used in different ice concentrations. While the technique was effective, the mean speed through the ice was lower than all other participants.

Operators with experience operating the lifeboat in previous experiments appeared to operate the lifeboat at higher speeds in lower concentrations and overall used a higher throttle in pack ice conditions. In post-trial interviews with the experienced operators, they noted they were less concerned with the integrity of the lifeboat due to their comfort impacting the ice at speeds greater than 0.5 m/s based on their previous experience. They also believed the motions of the vessel were not significant enough to disrupt crew comfort as long as the vessel did not experience high impact forces.

5.4.2 Effect of Operating Styles on Extreme Local Ice Pressure

Observations from field trials indicated that there were different tactics used by lifeboat coxswains who had experience operating small craft compared to the coxswains who had experience operating larger vessels. The analysis of ice load magnitudes resulting from testing in a given ice concentration highlighted that these loads varied because different coxswains had different background experience and used different navigational tactics. More aggressive navigational strategies lead to the lifeboat being exposed to a larger quantity of ice loads during a given test, which could affect the design load estimation. An example is provided below to illustrate how this operational consideration can be linked to extreme loads. In general, the radar plots depict that the magnitude of ice loads were relatively high for coxswain EL1, who had the most aggressive operating style, when compared to the other coxswains. On the other hand, coxswain LV3 used a conservative approach to maneuver the lifeboat, cautiously weaving through gaps between ice floes resulting in a lower magnitude of ice loads during impacts. This operational tactic may be due to coxswain LV3's experience as an icebreaker captain. Figure 5.10 shows a comparison of local ice pressure curves for two different coxswains. Both coxswains operated the lifeboat in similar ice conditions, but used different operating styles.
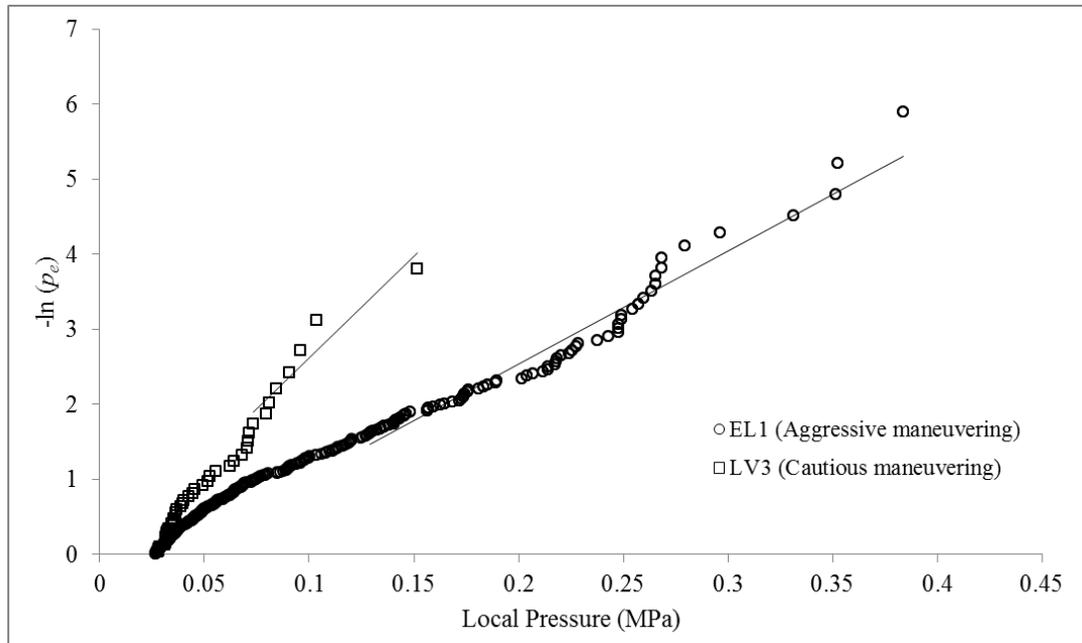
Figure 5.10: Local pressure curve for impact events on the stem for two different operating styles

It is clear that these two local ice pressure curves have distinct features. These distinct features relate to different design parameter values, which are listed in Table 5.2 for both cases. The magnitudes of both the α value and the x_o value are significantly higher in the aggressive maneuvering coxswain when compared to the cautious maneuvering coxswain. As these parameters govern the extreme pressure, the aggressive maneuvering coxswain would result in a larger extreme load.

Table 5.2: Parameters estimated from the local pressure curves (2013 stem loads)

Operating styles	Stem loads 2013	
	α	x_0
EL1 (Aggressive maneuvering)	0.066 MPa	-0.032 MPa
LV3 (Cautious maneuvering)	0.037 MPa	-0.003 MPa

From the tests data, the approximate number of impacts per kilometer sail-away distance was 800 and 260 for EL1 and LV3, respectively. It is evident that the expected number of impacts will be increased radically when the coxswain employs an aggressive operating style. An increased number of impacts will result in a higher local extreme pressure calculation. Table 5.3 summarizes the estimated extreme pressures for the two operating tactics (aggressive versus cautious) using the event-maximum method. The estimated extreme pressure for the aggressive case is almost twice that for the cautious case, indicating that the type of navigational tactic can play a large role in design requirements for lifeboats. This operational finding could be used to train lifeboat coxswains to navigate using methods that would prevent large ice loads and thus reduce potential structural damage and injury of personnel.

Table 5.3: Extreme pressures at stem based on different maneuvering strategies

Transit distance (km)	Stem extreme pressures (MPa) for two different operating styles and transit distances	
	EL1 (Aggressive maneuvering)	LV3 (Cautious maneuvering)
0.5 km	0.63	0.32
1.0 km	0.67	0.35
5.0 km	0.78	0.41

As discussed in the previous chapter, the lifeboat must be able to withstand all such loads to prevent an untrained or less experienced coxswain from damaging the lifeboat, but training effects should highlight the importance of maneuvering strategy on loads and ultimately the safety of the lifeboat.

5.4.3   Training Applications

The study shows that different techniques influence the ability of the operator to maneuver through ice at speed and that some tactics affect vessel loads and motions. These results can be applied to training programs to illustrate the influence of different behaviors, as well as to train operators to use different techniques in specific situations. As an example, if the coxswain is in a scenario where the strategy is to minimize forces and motions on the vessel and there is no immediate hazard, then s/he may wish to operate like operator LV3. Alternatively, if there is an emerging hazard that requires a quick escape from the platform, the coxswain may wish to operate like operator EL1, accepting the higher risk of vessel damage or crew discomfort. In high ice concentrations, achieving a high mean speed may not be achievable, and instruction may focus on techniques that allow the operator to progress through the ice safely rather than achieving a high mean speed. Depending on the training objective that is being taught, such as achieving speed or maintaining vessel integrity, trainers can tailor their teaching approach accordingly. Practical recommendations may also necessitate that longer air supplies be required for lifeboats in ice as longer times will be needed to navigate to the safety zone.

In an emergency situation involving an evacuation of the lifeboat into ice, the coxswain will be faced with decisions regarding the influence of maneuvering techniques on the ability to perform successfully. Depending on the severity of the hazard, the coxswain may be required to move to a safe zone very quickly. In this case, an aggressive approach may be needed, and crew comfort and vessel integrity may become secondary to moving quickly away from the hazard. In other cases the operator may need to use special

techniques to move through higher ice concentrations. Consideration needs to be given to the type and size of ice that may be encountered. While forces measured in the present study were low due to the size of the ice used in the tests, the study shows that different approaches result in different impact forces. Operator training program can provide the structural limitations of the lifeboat and how impacting large ice flows at high speeds increase the risk of vessel damage.

6 Conclusion

6.1 Original Contributions

Full scale local impact loads measured at two locations on an instrumented TEMPSC were analyzed using the event-maximum method of local pressure estimation to improve understanding of the nature of ice loads for such interactions and to evaluate the suitability of this approach for design load estimation for lifeboats and other GRP vessels in ice. High variability of ice loads has been observed and emphasis in the present work has been placed on the extreme pressures of interest for design. The pressure curve for impact events yielded values of α and x_0 parameters that produced conservative design estimates for the conditions considered in this analysis. The effects of the following factors on local pressure estimation have been discussed:

- The mean field ice concentration does not have a clearly defined effect on the magnitude of ice loads; rather these loads depend on the local variation of ice concentration and how the vessel was impacting with ice (e.g. straight line impact). There are more chances for higher peak loads to occur in higher ice concentration due to the impact with two or more ice floes that were packed together and less area available for pushing away the floes. From the data, it was found that most of the high magnitude peak loads occurred at the stem area of the vessel due to straight line impacts with ice. In addition, the vessel is more exposed in higher ice concentration, which results higher number of impacts. These are the considerations that lead to the increase of estimated local pressure with increasing ice concentration.

- This method investigated two different ice floe mass cases (similar floe size, but different thickness). Heavier ice blocks were observed to transmit significantly higher loads on the lifeboat as the lifeboat-ice interactions are highly influenced by kinetic energy.

- The stiffness of the vessel plays a significant role on the magnitude of peak loads measured on the panels. GRP panels are expected to impart lower peak force than steel structures due to the dissipation of energy over a longer time deflection. This is an important consideration when applying this method for local pressure estimation. This also highlight that the parent distributions for experimental data sets such as these are only representative of that structure and ice conditions considered. Caution must be exercised in applying such data to other, significantly different circumstances. For example, load estimated for larger, stiffer vessels could be less conservative if these estimates are based on the present data.

The overall distribution of ice loads were also presented in this thesis. These operational ice load models provide guidance to the general characteristics of ice loads measured on composite structure vessels operating in certain ice conditions.

The effect of coxswain's experience and the type of navigational strategies employed by different coxswains on the design load limits and other operational performance benchmarks have been investigated. This operational finding could be used to train lifeboat coxswains to mitigate large ice loads and thus reduce potential structural damage

and injury of personnel. In addition, this work will provide operational guidance towards other elements of lifeboat performance, including the transiting distance in a given ice conditions. From this study, it is also found that the lifeboats operating in high ice cover will need longer time to escape to the exclusion zone and should be fitted with larger compressed air supplies.

The research presented in this thesis can support the development of rational design methods, which aim to link design loads with the environmental and operating conditions that the lifeboat or any other small GRP vessels will be exposed. These tools will provide designers with greater confidence and flexibility in extending existing technology and developing new solutions for these regions.

6.2   Recommendation for Future Research

The followings are recommended for future work:

- It is clear that the effects of vessel mass, ice floe mass, and vessel speed on the interaction dynamics are complex and not well understood. Additional data including larger and stiffer vessels, and larger ice floes are needed, particularly for those to be deployed from existent platforms.

- The effect of ice strength on ice loading is not investigated as the tests were conducted in similar type of ice (fresh water ice). During testing, most of the impact energy transmitted to the ice floes, which were pushed away by the lifeboat.

Consequently the local ice crushing event was negligible. As ice floe and vessel sizes increase, the limiting condition will also change and crushing strength will become an increasingly important limit on ice loads transmitted to the vessels.

- No pressure-area relation can be developed from this study as the loads were measured only on two different load panels. Further work is recommended to measure the ice loads on several locations of the vessel having different panel areas to establish such design pressure-area relation.

- Conducting full scale experiments is expensive and not easy to do. Numerical modeling of ice loads for GRP vessels can be performed and this model can be compared with these field test data. It is recommended that emphasis be placed on gaining insights into the vessel response to ice loads.

Bibliography

Barker, A., Simões Ré, A., Walsh, D., and Kennedy, E., 2004. Model Testing of an Evacuation System in Ice-Covered Waters with Waves, PERD/CHC Report 61-6, 92 pages.

Billard, R., Rahman, M. S., Kennedy, A., Simões Ré, A., and Veitch, B., 2014. Operability of lifeboats in pack ice: coxswains' skill and design factors. Proceedings of Arctic Technology Conference, Houston, Texas, OTC 24610.

Browne, R. P., Gatehouse, E. G., and Reynolds, A., 2008. Design of an Ice Strengthened Lifeboat. Proceedings of ICETECH 2008, 8 pages.

Frederking, R., 2003. Determination of Local Ice Pressures from Ship Transits in Ice. Proceedings of the Thirteenth International Offshore and Polar Engineering Conference, Honolulu, Hawaii, USA.

Ice Navigation in Canadian Waters, 2012. Minister of Fisheries and Oceans Canada, 165 pages.

Igloliorte, G., Kendrick, A., and Fredj, A., 2007.Global and Structural Performance of a TEMPSC in Pressured Ice. Proceedings of the 26th International Conference on Offshore Mechanics and Arctic Engineering (OMAE), 14 pages.

Igloliorte, G., Kendrick, A., Brown, R., and Boone, J., 2008. Performance Trials of a Totally Enclosed Motor Propelled Survival Craft, Proceedings of ICETECH 2008, 9 pages.

International Maritime Organization (2007) Guidelines for Ships Operating in Polar Waters – Annex 11, 36 pages.

International Organization for Standardization (ISO) Petroleum and Natural Gas Industries – Arctic Offshore Structures, 19906: 2011.

Johansson, B. M., 2006. Ice Breaking Life Boat, Proceedings of ICETECH 2006, Paper Number ICETECH06-162-RF.

Jordaan, I. J., Maes, M. A., Browne, P. W., and Hermans, I. P., 1993, "Probabilistic Analysis of Local Ice Pressures," ASME J. Offshore Mech. Arct. Eng., 115, pp. 83–89.

Kennedy, A., 2010. Limitations of Lifeboats Operating in Ice Environments. M. Eng. Thesis, 170 pages.

Kennedy, A., Simões Ré, A., and Veitch, B, 2010. Operational Limitations of Conventional Lifeboats Operating in Sea Ice. Proceedings of ICETECH 2010, Anchorage.

Kennedy, A., Simões Ré, A., and Veitch, B., 2014. Peak Ice Loads on a Lifeboat in Pack Ice Conditions. Proceedings of Arctic Technology Conference, Houston, OTC 24608.

Kennedy, A. and Simões Ré, A., 2013. 2013 Ice Trials – TEMPSC Operation in Pack Ice. OCRE-TR-2014-022, 33 pages.

Kennedy, A. and Simões Ré, A., 2014. 2014 Ice Trials – TEMPSC Limitations in Pack Ice Conditions. OCRE-TR-2014-025, 101 pages.

Lau, M. and Simões Ré, A., 2006. Performance of Survival Craft in Ice Environments. Proceedings of ICETECH 2006, 8 pages.

"Li, C., Frederking, R., and Jordaan, I., Simulation of Probabilistic Averaging in Ice Load Estimation. Proceedings of the 18th IAHR InternationalSymposium on Ice, 8 pages.

LSA, 2010. Life-Saving Appliances – Including LSA Code. International Maritime Organization, London.

Popov, Y. N., Faddeyev, O. V., Kheysin, D. Y., Yakovlev, A. A., 1968. Strength of Sailing Ships in Ice. Sudostroyeniye Publishing House, Leiningrad, 223 pages.

Rahman, M. S., Taylor, R. S., Simões Ré, A., Kennedy, A., Wang, J., and Veitch, B., 2014. Probabilistic Analysis of Local Ice Loads on a Lifeboat. ICETECH14-104, Banff, Alberta, Canada.

Scott, R. J., 2010. Fiberglass Boat Design and Construction. Published by the Society of Naval Architects and Marine Engineers, 2nd edition, ISBN 0-939773-19-8, 140 pages.

Seligman, B., Bercha, F., and Hatfield, P., 2008. ARKTOS Full-Scale Evacuation Tests. Proceedings of ICETECH 2008, 6 pages.

Simões Ré, A. and Veitch, B., 2003. Performance Limits for Evacuation Systems in Ice. Proceedings of Port and Ocean Engineering under Arctic Conditions, Trondheim.

Simões Ré, A. and Veitch, B., 2007. Lifeboat Operational Performance in Cold Environment. Royal Institution of Naval Architects (RINA) International Conference, 6 pages.

Simões Ré, A. and Veitch, B., 2008. Escape-evacuation-rescue Response in Ice-covered Regions. Proceedings of International Offshore and Polar Engineering Conference, Vancouver.

Simões Ré, A., Kuczora, A., and Veitch, B., 2008. Field Trials of an Instrumented Lifeboat in Ice Conditions. Proceedings of Offshore and Polar Engineering Conference, Vancouver.

Simões Ré, A., Veitch, B., Kuczora, A., Barker, A., Sudom, D., and Gifford, P., 2011. Field Trials of a Lifeboat in Ice and Open Water Conditions. Proceedings of Port and Ocean Engineering under Arctic Conditions, Montréal.

Simões Ré, A. and Veitch, B., 2012. Evacuation in Ice: Field Trials of a Conventional Lifeboat in Pack and Level Ice. Proceedings of Arctic Technology Conference, OTC 23705, Houston.

Simões Ré, A. and Veitch, B., 2013. Evacuation In Ice: Ice Loads On a Lifeboat During Field Trials. Proceedings of Offshore Mechanics and Arctic Engineering, OMAE2013-10689, Nantes.

Simões Ré, A., Veitch, B., Gifford, P., Kennedy, E., Kirbi, C., Kuczora, A., and Sudom, D., 2012. Performance and Survivability of Totally Enclosed Motor Propelled Survival Craft (TEMPSC) in Ice and Open Water Conditions. Report number. OCRE-TR-2012-07.

Sudom, D., Kennedy, E., Ennis, T., Simões Ré, A., and Timco, G. W., 2006. Testing of Evacuation System Models in Ice-covered Water with Waves. Canadian Hydraulic Centre Report CHC-TR-37, Ottawa, 41 pages.

Suyuthia, A., Leiraa, B. J., and Riska, K., 2012.Statistics of Local Ice Load Peaks on Ship Hulls. Journal of Structural Safety (2013) 1-10, Elsevier, 10 pages.

Taylor, R. S., Jordaan, I. J., Li, C., and Sudom, D., 2010. Local Design Pressures for Structures in Ice: Analysis of Full-scale Data. Journal of Offshore Mechanics and Arctic Engineering. Vol. 132 / 031502-1.

The UK Health and Safety Executive, 2007. TEMPSC Structural Design Basis Determination - part 1, 2, and 3.

Timco, G. W and Dickins, D. F., 2005. Environment Guidelines for EER Systems in Ice-Covered Waters. Cold Regions Science and Technology 42 (2005) 201 – 214.

Standards for Lifeboats, Transport Canada TP 7320 E, 1992, 62 pages.

Wright, B.D., Timco, G.W., Dunderdale, P., and Smith, M., 2002. Evaluation of Emergency Evacuation Systems in Ice-covered Waters. PERD/CHC Report 11-39.

Wright, B., Timco, Garry, Dunderdale, P., and Smith, M., 2003. An Overview of Evacuation Systems for Structures in Ice-Covered Waters. Proceedings of the Port and Ocean Engineering under Arctic Conditions, Trondheim, Norway, Vol. 2, pp 765-774 .